

SIMGRO 7.2.9

Theory and model implementation

**P.E.V. van Walsum
A.A. Veldhuizen
P. Groenendijk**

Alterra-report 913.1

Alterra, Green World Research, Wageningen

ABSTRACT

P.E.V. van Walsum, A.A. Veldhuizen, P. Groenendijk, 2011. *SIMGRO 7.2.9, Theory and model implementation*. Wageningen, Alterra. Alterra-Report 913.1. 93 pp.

SIMGRO is a modelling framework that can facilitate the investigation of various kinds of regional water management problems. The framework connects to diverse hydrologic model codes like MODFLOW for groundwater and SOBEK-CF for surface water simulation. A number of 'in-house' codes make SIMGRO especially suitable for modelling situations with shallow groundwater levels in relatively flat areas, like in delta regions. The 'metamodel' MetaSWAP is based on a quasi steady-state solution of the Richards' equation. Its implementation can include crop growth simulation with WOFOST, with feedback to the hydrologic parameters like root zone depth and leaf area index. The SIMGRO package also includes a simplified code for the simulation of surface water processes. A special feature of the framework is the option for model coupling via a shared state variable that is alternately updated by the connected models.

Keywords: integrated water management, mechanistic, distributed, dynamic, saturated-unsaturated flow, surface water, drainage; semi-implicit

ISSN 1566-7197

© 2012 Alterra,
P.O. Box 47, NL-6700 AA Wageningen (The Netherlands).
Phone: +31 317 474700; fax: +31 317 419000; e-mail: info.alterra@wur.nl

No part of this publication may be reproduced or published in any form or by any means, or stored in a data base or retrieval system, without the written permission of Alterra.

Alterra assumes no liability for any losses resulting from the use of this document.

Contents

Preface	5
1 Introduction	7
2 Plant/soil-atmosphere interactions	15
2.1 Introduction	15
2.2 Precipitation	15
2.3 Interception by vegetation canopy	16
2.4 Evapotranspiration (<i>Text in revision</i>)	20
2.5 Data summary	22
3 Soil water	23
3.1 Introduction	23
3.2 Ponding water and infiltration	24
3.2.1 Theory	24
3.2.2 Implementation	25
3.3 Unsaturated flow	30
3.3.1 Theory	30
3.3.2 Implementation	37
3.4 Coupling to regional groundwater flow	42
3.4.1 Theory	42
3.4.2 Implementation	44
3.5 Data summary	50
4 Drainage	51
4.1 Introduction	51
4.2 Theory	51
4.3 Model implementation	57
4.4 Data summary	61
5 Surface water	63
5.1 Introduction	63
5.2 Theory	63
5.3 Model implementation	64
5.3.1 Schematization and hydraulic metafunctions for channel flow	64
5.3.2 Dynamics of channel flow	67
5.3.3 Water on the soil surface	71
5.4 Data summary	74
6 Water management	75
6.1 Introduction	75
6.2 Land use	75
6.2.1 Urban areas	75
6.2.2 Sprinkled crops	76

6.3	Surface water	78
6.3.1	Weirs	78
6.3.2	Surface water supply links	79
6.3.3	Discharge pumps	80
References		81
Appendix A Steady-state unsaturated flow simulations		85

Preface

In the past year the model has been made suitable for soils with deep groundwater levels; formerly the evapotranspiration of such soils was underestimated. The added extra ‘aggregation layer’ for the zone just below the root zone remedied that deficiency. The idea of using extra aggregation layers was first suggested by former colleague Pim Dik. This idea has now been implemented in a generalized form, involving N-layers forming a cascade of nonlinear reservoirs.

The second major enhancement of the last year was the coupling to the crop growth model WOFOST. This coupling has been implemented in a two-way fashion, including the (optional) feedback from the vegetation development to the hydrologic model. The used state variables for this feedback are the depth of the root zone, the crop height, the leaf area index, and the soil cover. For facilitating this feedback an option was included for dynamic development of the root zone layer in MetaSWAP. The coupling to WOFOST coincided with the enhancement of the SWAP-WOFOST coupling by SWAP developers Joop Kroes, Jos van Dam and the WOFOST expert Iwan Supit. They provided the information needed for realizing the coupling of WOFOST to MetaSWAP.

The concept for the interception evaporation was reformulated, in collaboration with the SWAP developers. Furthermore, the SWAP-method for handling the partitioning between transpiration and soil evaporation was implemented. The Maas-Hoffman method was included for simulating the effect of salt stress on the transpiration uptake. The coupling to the TRANSOL model for simulating solute movements and processes in soils was implemented in collaboration with Joop Kroes. The program `metaswap2transol` also includes the temperature simulation of SWAP.

Low-cost parallel computing is now possible on multi-core pc’s with 2 to 8 cores. And high-performance pc-clusters provide a further multiplication of computing power. To make use of these opportunities the codes of MetaSWAP and SIMGRO-drainage have been parallelized via the OpenMP-protocol in combination with a state-of-art 64bit-compiler (Intel Fortran 11.1).

SIMGRO has a history that goes back to the mid-eighties. The first and second versions were developed by Erik Querner in collaboration with Jan van Bakel. In the course of time, various other persons not belonging to the current team have contributed in one way or the other: Pim Dik, Robert Smit, and Frank van der Bolt.

The realization of SIMGRO7 was financed by the National Hydrologic Instrument project, by the Centre for Water & Climate of Alterra-Wageningen UR, by the Alterra funds for strategic research, and by the GENESIS project of 7th EU Framework program.

Wageningen, December 2009.

1 Introduction

All regional hydrologic models suffer the deficiency that the hydrologic cycle is not fully simulated in all its processes and dimensions. In the first place this concerns the spatial limitation of a model, which necessitates the making of assumptions with respect to external boundary conditions. Furthermore, most models cover only part of the processes *within* a region. The remedy is to then introduce internal boundary conditions. But these conditions are more often than not a gross schematization of reality, lacking essential feedback mechanisms. To some degree, that even applies to the commonly used assumption that the precipitation and evaporative demand of the atmosphere can be seen as external boundary conditions: the larger the basin, the less this assumption is valid. For coming to grips with many issues of integrated water management, it is necessary to have a model code that covers the whole (regional) system, including plant-atmosphere interactions, soil water, groundwater and surface water. SIMGRO (a dated acronym of SIMulation of GROundwater, Querner and Van Bakel, 1989, Veldhuizen *et al.*, 1998) was developed for that purpose.

The name ‘SIMGRO’ was formerly used for referring to an integrated model code, including submodels for the compartments and processes as shown in Figure 1. Now it is used in the meaning of a modelling framework. This framework has been connected to a number of ‘in-house’ components, but also has possibilities for coupling to other codes. The in-house components are indicated in the form of chapter numbers in the overall scheme of regional water flows given in Figure 2. They can be grouped as follows:

- an SVAT-model that is commonly referred to as ‘MetaSWAP’, covering the plant-atmosphere interactions and soil water;
- a simplified surface water metamodel;
- a drainage package, for simulating groundwater drainage with fast feedback from surface water.

Figure 1 Schematization in SIMGRO of the hydrologic system by integration of saturated zone, unsaturated zone and surface water (Querner and van Bakel, 1989).

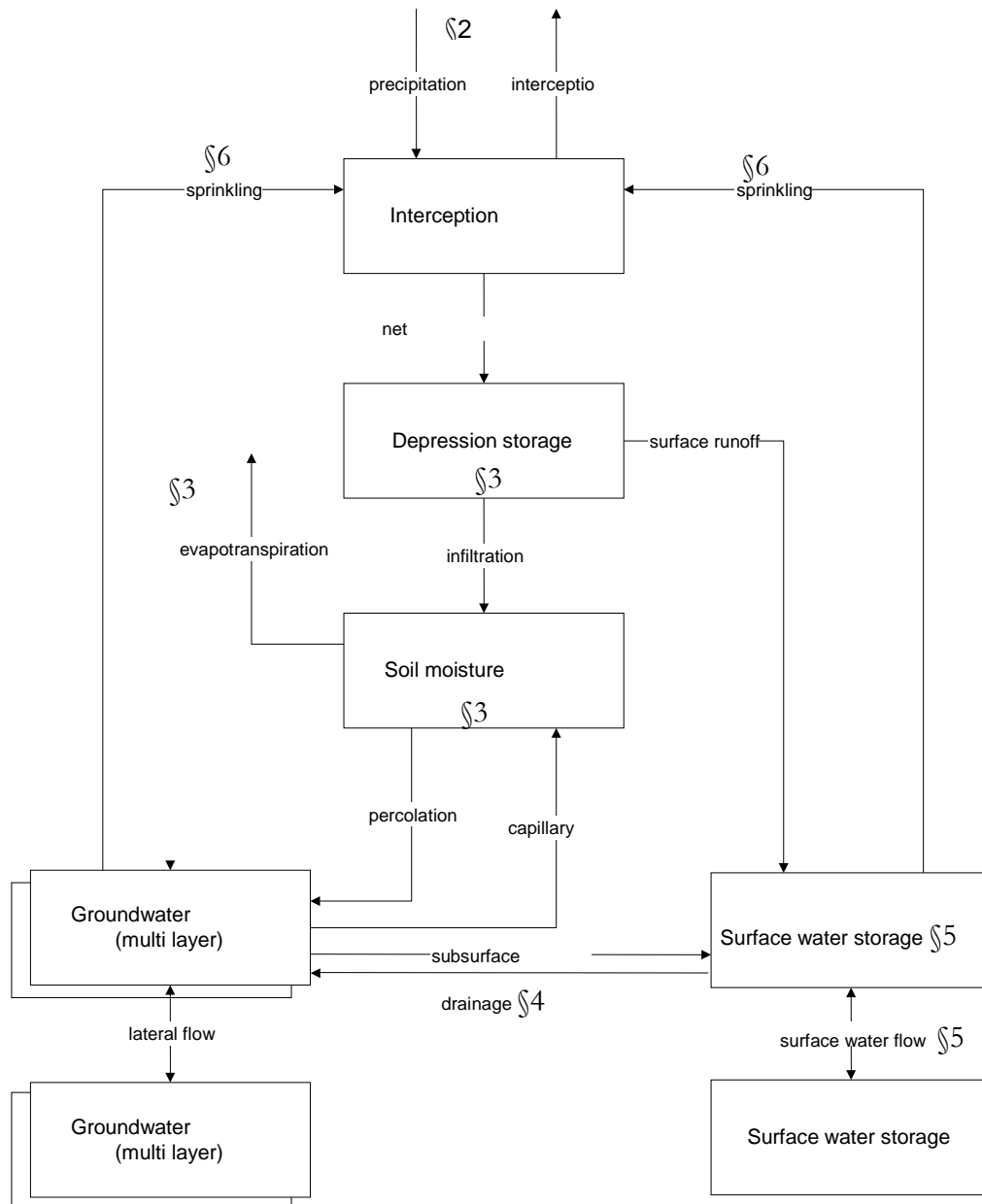


Figure 2 Schematization of regional water flows by means of transmission links and storage elements. The flows and links that can be modelled with in-house components are indicated with §- references. For groundwater (MODFLOW) and surface water (SOBEK-CF) there are connectors for external models.

The current possibilities for coupling to other codes are:

- MODFLOW for groundwater;
- SOBEK-CF for surface water.

SOBEK-CF can be used in combination with the simplified surface water metamodel, with the latter implemented for the upstream waterways and SOBEK-CF for the larger downstream ones. The current software implementation still involves couplings to *specific* external codes. But the way in which this has been done makes it a relatively small step to arrive at a 'component-based' implementation that allows connections to any code that is 'OpenMI-compliant' (i.e. compliant with 'Open Modelling Interface', HarmonIT, 2005). This software migration to an OpenMI-compliant version of SIMGRO is planned for the near future.

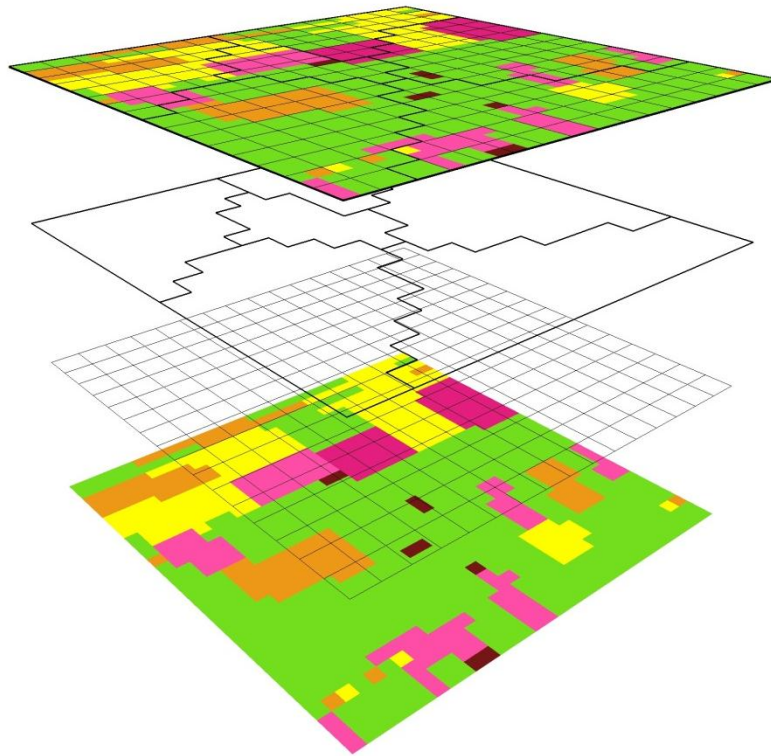


Figure 3 Example of how the spatial schematisations of an integrated model can be constructed. The bottom layer involves the units obtained from an overlay of the land use and soil maps. The next layer represents the cells of the groundwater model, followed by the subcatchments of the surface water model in the next layer. The top layer shows how the schematisations have been combined. If there is just one colour in a groundwater cell, then there is just a single SVAT-unit linked to it. If there are more colours, then two or more SVAT units are connected.

Connections between models are in SIMGRO defined in terms of *mapping tables*, as is done when using OpenMI technology. Each record of such a table contains a pair of 'identifiers' that define an '*id*-based' link between two models. In Figure 3 an example is given of how a model schematisation can be built and then coded in the form of these *id*-based links. In the case that a grid cell in the top layer of the figure contains more than one colour, then two or more SVAT units are connected to a single groundwater cell. This is the so-called *N:1* coupling. In the shown schematisation there is also an *N:1* coupling between the SVAT's and the subcatchments of the surface water model.

SIMGRO has two options for connections between models:

- a flux-based link, *q*-link;
- a head-based link, *h*-link.

Flux-based links are the type generally used in combination with OpenMI technology. In such a link between 'Model A' and Model 'B', the first computes an exchange flux. If this flux is based on a single cycle of model interaction, then the scheme is called 'explicit'. With this method two types of related problems can occur:

- the flux causes Model B to run dry, causing a water balance error if Model A still assumes that the water is available;
- the flux causes a large disturbance of the head simulation in Model B, which in the next cycle leads to destabilization of the model combination, involving oscillatory behaviour of the flux.

In order to avoid water balance errors, a flux-based link can be made to include a *put* and a *get* operation. In the *put*-step the Model A sends a demand to Model B in the form of a flux. That model then checks whether the water is available, and determines the *demand realisation*, which is then returned in a *put* by B. The realisation is then picked up via a *get* by Model A. The destabilization problem can be solved by including an iteration cycle. Such a cycle will also remedy any water balance errors, if allowed to fully converge. In that case the coupling method is called ‘implicit’.

In SIMGRO, the put/get cycle is used for the flux-based coupling between MetaSWAP and a surface water model. In the case of a $N:1$ coupling, the demands are first totalized. On return of the realisation, this is then distributed by SIMGRO over the units that placed the demand (Figure 4). The iterative coupling is only used for a flux-based link between MetaSWAP and MODFLOW.

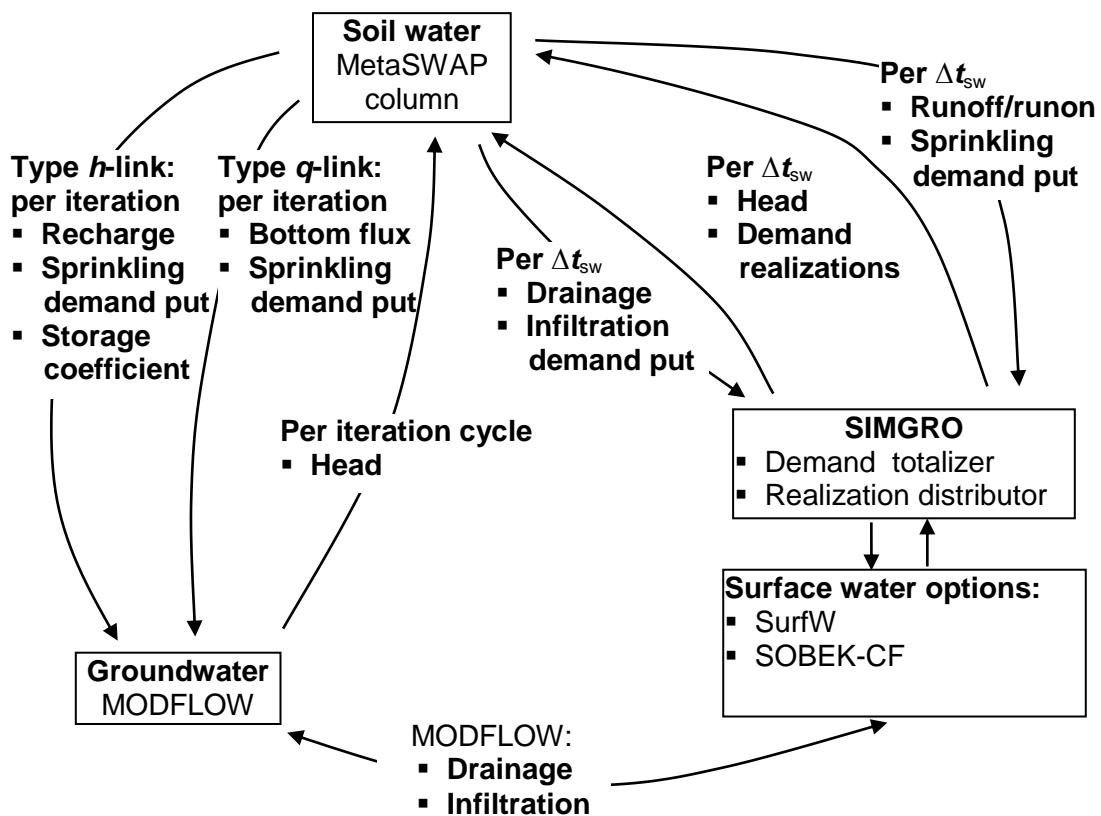


Figure 4 Modules with relationships and options. MetaSWAP is the in-house “SVAT” (Soil-Vegetation-Atmosphere Transfer) model of SIMGRO. SurfW is the in-house surface water metamodel. It can be used in combination with the hydraulic model SOBEK-CF. The links involve the ‘putting’ of demands and the reply in the form of a ‘demand realization’. The left half of the scheme has a time step of the groundwater model, Δt_{gw} , the right half of the ‘fast processes’, Δt_{sw} .

A so-called *h*-link is a special feature of the SIMGRO framework, involving the head as a *shared state variable* of two connected models. The shared variable is alternately updated by Model A and Model B. This is done in the following two substeps:

- an ‘explicit’ substep by Model A;
- an ‘implicit’ substep by Model B, using information obtained in the first substep.

In the second substep the assumption is that the fluxes of the first substep remain unchanged. Under this assumption, the second substep for Model B only affects Model A in terms of its water storage. In order to take this into account in the second substep, the first substep also provides the relationship between the shared state variable and the storage in Model A. The storage relationship is included in the set of equations that is to be solved in the implicit scheme of Model B in the second substep.

In an ‘explicit’ scheme the fluxes between the models are purely determined by the update of Model A. But in the *b*-link scheme the total fluxes between the connecting models are determined from budget calculations after Model B has been updated. This is what distinguishes the method from a purely explicit one, and justifies calling it ‘semi-implicit’.

For the MetaSWAP-MODFLOW coupling the *b*-link is the most used method, because it makes the phreatic level available to MODFLOW: the *b*-link can be seen as a *q*-link between the phreatic level and the MODFLOW head, with a flow resistance that approaches zero. The MODFLOW head can then be used as the phreatic level in the MODFLOW drainage packages (*RIV*, *DRN*, etc.).

For the MetaSWAP-SurfW modelling the *b*-link is used for the runoff/runon simulation, because the low resistance of this flow process would otherwise require very small time steps or a computationally demanding iterative implicit scheme to avoid destabilization of the model combination.

As can be seen from the overview in Figure 4, SIMGRO has separate time steps for the ‘fast’ processes (Δt_s) and for the ‘slow’ ones (Δt_g). The ‘fast’ processes include plant/atmosphere interactions, flow over the soil surface, drainage with surface water feedback, and channel flow. Soil water and groundwater flow are modelled as ‘slow’ processes. Typical time steps used in the current modelling practice are $\Delta t_s = 1$ hour and $\Delta t_g = 1$ day.

In the flow chart with an overview of the SIMGRO modelling cycles given in Figure 5, the fast time step is present in the top half, and the slow step in the bottom half. The iteration cycle around the groundwater model is needed because most groundwater models can not handle a nonlinear storage relationship. (By contrast, all surface water models have such a facility.). In the software implementation of the coupling scheme, the recharge is passed to the groundwater model along with the storage coefficient, for each iteration cycle. But the recharge is in fact only updated once per *groundwater time step* by the MetaSWAP model itself. In the case of a *q*-link, however, the bottom flux *is* updated for every iteration cycle.

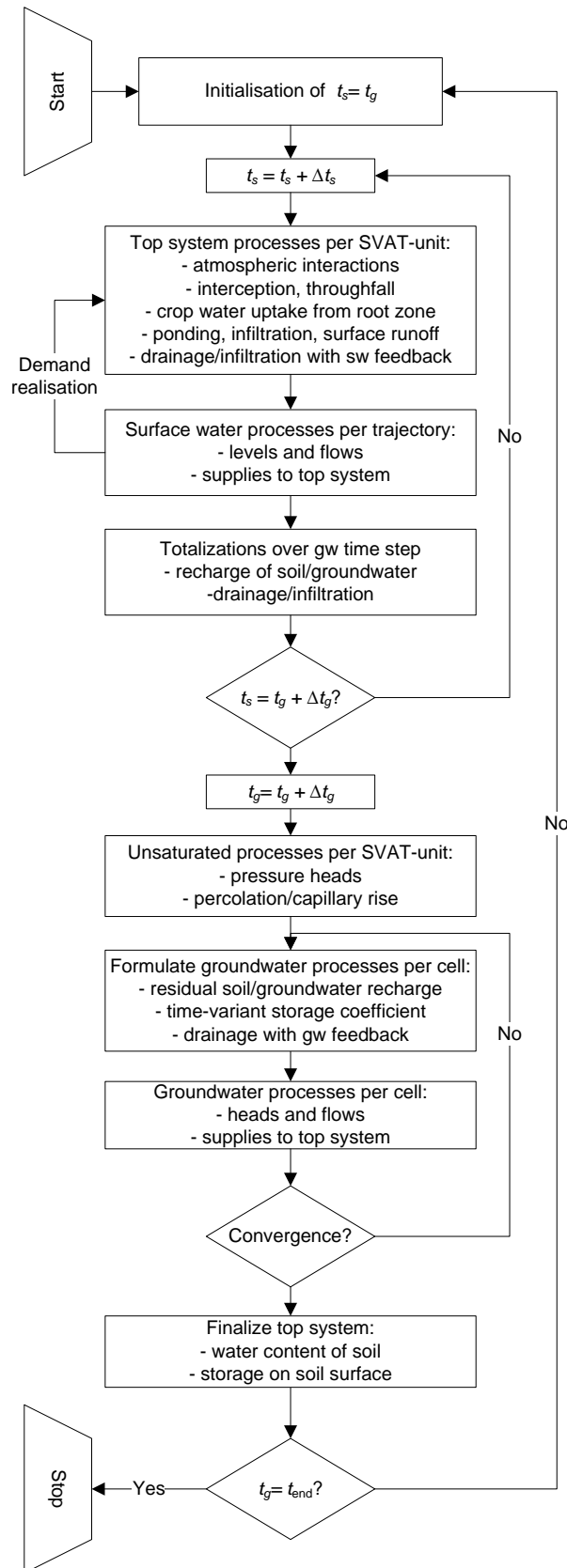


Figure 5 Overview of modelling cycles. The time variable of the fast top-system processes t_s is synchronized with t_g of the groundwater processes at the beginning of each groundwater time step. The 'residual' soil/groundwater recharge is the remaining column recharge after discounting the water needed for updating the pressure heads. Water management is not shown.

The simulation of (possible) changes in water management is the goal of most studies. Given its crucial importance for the practical relevance of the model, the management options are described in a separate section (§6). But of course the distinction between what is considered ‘water management’ and what ‘natural functioning’ depends on the perspective that one has. Here any type of land-use involving vegetated soil is considered to be ‘natural’, even though it is some form of agriculture. In the case of land-use, the term water management is reserved for paved areas, involving some form of interference in the cycle, e.g. urban areas. The layout of man-made ditches is described as if it were part of the natural system, whereas it is of course not. In the case of surface water the term ‘management’ is reserved for the manipulation of the water flows and levels through the use of structures.

In the following sections a description is given of the used conceptualizations, followed by more detailed descriptions about the way they have been implemented. To aid the reader in quickly locating the descriptions, the overview in Figure 2 has been furnished with hyper-links to the subsections.

2 Plant/soil-atmosphere interactions

2.1 Introduction

Interactions with the atmosphere are the drivers of the regional system. The recharge is sensitive to the water balance of precipitation and evapotranspiration: a relative error or change in either of these terms is amplified by a factor 2-3 in the computation of the recharge.

Most regional hydrologic models do not take into account the feedbacks to the atmospheric system. But the larger the scale of the model application, the less valid this simplification becomes. In the methods described below we do not take the feedbacks into account; but (for the evapotranspiration) we do give some consideration to the consequences of this choice and about how to minimize the involved modelling error.

2.2 Precipitation

It is well known that the measurement of precipitation usually contains systematic errors due to wind-effects. The size of the error is usually in the order of a few % (<5%), but should be accounted for. The 'natural' precipitation can be augmented by sprinkling. The total (gross) precipitation is then given by:

$$P_g(t) = P(t) + P_{s,n}(t) \quad (1)$$

where:

$$\begin{aligned} P_{gr}(t) &= \text{gross precipitation rate at time } t \text{ (m}^3 \text{ m}^{-2} \text{ d}^{-1}\text{)} \\ P(t) &= \text{natural precipitation rate at time } t \text{ (m}^3 \text{ m}^{-2} \text{ d}^{-1}\text{)} \\ P_{s,n}(t) &= \text{net sprinkling rate at time } t \text{ (Eq. 80) (m}^3 \text{ m}^{-2} \text{ d}^{-1}\text{)} \end{aligned}$$

In the above relationship (and in others for the processes at or around the soil surface) we use the dimension $[L^3L^{-2}]$ when the value per-unit-of-area is meant. After multiplication by the relevant area fraction the *spatial mean* is obtained in $[L]$. Not in all cases this distinction is relevant; we then use the latter notation.

The time dependency of the precipitation (and other variables representing atmospheric boundary conditions) is averaged over the used simulation interval. For this the interval Δt_s of the 'fast' processes is used. The use of time-averaged values is indicated via the superscript 'ave'. So Eq. 1 then becomes:

$$P_g^{ave} = P_g + P_{s,n}^{ave} \quad (2)$$

where:

$$\begin{aligned} P_g^{ave} &= \text{gross precipitation rate, time averaged for interval (m}^3 \text{ m}^{-2} \text{ d}^{-1}\text{)} \\ P^{ave} &= \text{natural precipitation rate, time averaged for the interval (m}^3 \text{ m}^{-2} \text{ d}^{-1}\text{)} \\ P_{s,n}^{ave} &= \text{net sprinkling rate, time averaged for the interval (m}^3 \text{ m}^{-2} \text{ d}^{-1}\text{)} \end{aligned}$$

2.3 Interception by vegetation canopy

Incoming precipitation (and/or sprinkling water) either falls directly on the ground surface – as free throughfall – or is intercepted by the vegetation canopy. Part of that interception directly splashes off at the impact. The part that does not, is subsequently stored on the canopy and evaporate, or else reach the ground surface as stemflow or drops from the leaves. We adapted the approach of Rutter *et al.* (1971). The relationship between the canopy interception evaporation and the degree of canopy saturation is a discontinuous function.

The interception reservoir has a maximum storage capacity that is strongly related to the leaf area and therefore depends on the season. It is much smaller than the soil storage capacity, i.e. in the order of a few millimetres at most. However, the fast interception dynamics involve frequent use of this capacity and thus the role in the hydrological cycle can be significant. To capture these dynamics it is important to use short time intervals. If the meteorological data have been obtained at 1 hour intervals, the filling and emptying of the reservoir can be adequately modelled in most cases.

The interception evaporation is modelled as a ‘diffuse’ vertical process, with no clear-cut division between vegetation cover and bare soil. Precipitation that comes into contact with the canopy - and that does not directly splash off - is denoted as the gross intercepted precipitation. It is modelled as a simple fraction of the gross precipitation:

$$P_{i,g}(t) = c_i P_g(t) \quad (A1)$$

where $P_{i,g}(t)$ is the gross intercepted precipitation as a function of time (m d^{-1}), $P_g(t)$ is the gross precipitation (rainfall plus sprinkling irrigation) (m d^{-1}), and c_i is the interception fraction. The interception water balance is simulated with:

$$\frac{dS_i(t)}{dt} = P_{i,g}(t) - E_i(t) - D_i(t) \quad (A2)$$

where $S_i(t)$ is the water stored in the interception reservoir (m), E_i is the canopy evaporation rate (m d^{-1}), and $D_i(t)$ is the canopy dripping rate (m d^{-1}). It is essential to use an analytical solution to the above equation, to avoid numerical errors caused by time discretization. That is then avoided if the time step is not larger than the gauging interval of the precipitation and the evaporative demand.

Dripping from the canopy starts when the canopy becomes saturated, any excess water directly drips through. The storage of water in the canopy is assumed to be bounded:

$$S_i(t) \leq S_{i,\text{cap}}(t) \quad (\text{A3})$$

where $S_i(t)$ is the water stored in the interception reservoir (m), and $S_{i,\text{cap}}(t)$ is storage capacity of the interception reservoir (m). The canopy evaporation rate is assumed to depend on the canopy saturation and the potential evaporation rate as:

$$E_i(t) = [f_{i,\text{min}} + (1 - f_{i,\text{min}}) \frac{S_i(t)}{S_{i,\text{cap}}}] E_{i,p}(t), \quad \text{for } S_i(t) > 0 \quad (\text{A4a/b})$$

$$E_i(t) = 0, \quad \text{for } S_i(t) = 0$$

where $E_{i,p}(t)$ is the potential evaporation rate of a wet canopy (m d^{-1}), and $f_{i,\text{min}}$ is the ‘start-up’ fraction of the canopy evaporation reduction factor (-). If $f_{i,\text{min}} = 0$ the relationship is linear like in Rutter (1971). For a value of 1.0 the evaporation rate equals the potential rate as long as there is water in the reservoir. The method to obtain the potential rate $E_{i,p}(t)$ is given in Eq. (6) in the main text.

In the solution scheme, the time variation of the precipitation rate is handled as a stepwise function. This is denoted by the superscript ‘ave’. The non-linear canopy evaporation rate relationship (Eq. A4) requires separate treatment for $f_{i,\text{min}}$ equal to unity.

Case 1: Discrete dependence of evaporation on canopy saturation

For $f_{i,\text{min}}$ equal unity (Eq. A4a), the following water balance can be made:

$$S_i^{j+1} = S_i^j + (P_{i,g}^{\text{ave}} - E_{i,p}^{\text{ave}}) \Delta t$$

$$S_i^{j+1} = \min(S_i^{j+1}, S_{i,\text{cap}}^{j+1}); \quad S_i^{j+1} = \max(S_i^{j+1}, 0) \quad (\text{A5})$$

where S_i^j (m) is the water stored in the interception reservoir at time level j , $P_{i,g}^{\text{ave}}$ (m d^{-1}) is the gross intercepted precipitation rate, time-averaged rate over interval Δt , and Δt (d) is the length of the simulation time interval.

In case that the reservoir does *not* become full, the evaporation follows from the balance:

$$E_i^{\text{ave}} = (S_i^j - S_i^{j+1})/\Delta t + P_{i,g}^{\text{ave}} \quad (\text{A6})$$

where E_i^{ave} (m d^{-1}) is the time averaged canopy evaporation rate. In this case the dripping rate is zero. In case the reservoir becomes full, the simulated evaporation rate equals the potential value during the *whole* interval owing to the discrete relationship of the canopy evaporation (potential value for a non-zero storage) and the use of time-averaged values:

$$E_i^{\text{ave}} = E_{i,p} \quad (\text{A7})$$

The net intercepted precipitation and the drip to the soil surface can now be found from:

$$\begin{aligned} P_{i,n}^{\text{ave}} &= (S_i^{j+1} - S_i^j)/\Delta t + E_i^{\text{ave}} \\ D_i^{\text{ave}} &= P_g^{\text{ave}} - P_{i,n}^{\text{ave}} \end{aligned} \quad (\text{A8})$$

where $P_{i,n}^{\text{ave}}$ (m d^{-1}) is the time averaged net intercepted precipitation and D_i^{ave} is time averaged the dripping rate. The equations above can also be used in case the potential canopy evaporation rate equals zero.

Case 2: Semi-continuous dependence of evaporation rate on canopy saturation

If $f_{i,\min}$ in Eq. (A4a) is less than unity, there is a semi-continuous dependence of the evaporation rate on the canopy saturation. After inserting the expression for the evaporation rate as given in Eq. A4a into Eq. (A2) and rearranging, we get for an unsaturated canopy ($S_i < S_{i,\text{cap}}$, $D_i=0$):

$$\frac{dS_i(t)}{dt} + \beta S_i(t) = \gamma, \quad \text{with } \beta = (1 - f_{i,\min}) \frac{E_{i,p}^{\text{ave}}}{S_{i,\text{cap}}} \quad \text{and } \gamma = P_{i,g}^{\text{ave}} - f_{i,\min} E_{i,p}^{\text{ave}} \quad (\text{A9})$$

Assuming that β is non-zero (see the above Case 2 for $\beta = 0$) and that the interception reservoir does not become full ($S_i < S_{i,\text{cap}}$, $D_c=0$), the solution to the differential equation for $S_i(t)$ is given by:

$$\begin{aligned} S_i^{j+1} &= (S_i^j - \frac{\gamma}{\beta})e^{-\beta\Delta t} + \frac{\gamma}{\beta} \\ S_i^{j+1} &= \max(S_i^{j+1}, 0) \end{aligned} \quad (\text{A10})$$

The **max**-operation prevents the interception storage from becoming less than zero. If the reservoir does not become full ($S_i < S_{i,\text{cap}}$) the evaporation is now given by Eq. A6.

If S_i (Eq. A10a) yields a value $> S_{i,\text{cap}}$ then we first determine the time at which this happens by solving for Δt_{cap} ($\Delta t_{\text{cap}} \leq \Delta t$):

$$S_{i,\text{cap}} = (S_i^j - \frac{\gamma}{\beta})e^{-\beta\Delta t_{\text{cap}}} + \frac{\gamma}{\beta}$$

$$\Delta t_{\text{cap}} = \frac{1}{\beta} \ln[(S_i^j - \frac{\gamma}{\beta}) / (S_{i,\text{cap}} - \frac{\gamma}{\beta})]$$
(A11)

where Δt_{cap} is the time to fill the reservoir during which there is no dripping from the canopy. The canopy evaporation can thus be found from a balance like the one given in Eq. A6; for the remaining part of the interval ($\Delta t - \Delta t_{\text{cap}}$) the evaporation rate is equal to the potential value. So the total canopy evaporation can be found from:

$$E_i^{\text{ave}} = \frac{1}{\Delta t} [S_i^j - S_i^{j+1} + \Delta t_{\text{cap}} P_{i,\text{g}}^{\text{ave}} + (\Delta t - \Delta t_{\text{cap}}) E_{i,\text{p}}^{\text{ave}}]$$
(A12)

The dripping rate then follows from Eq. A8.

2.4 Evapotranspiration (*Text in revision*)

An evapotranspiration simulation method should be accompanied by a method that provides acceptable parameters for the intended user community. In our case we used the crop coefficients given by Feddes (1987). Those coefficients, however, are intended for an ‘all-in-one’ evapotranspiration simulation method that does account for variable feedbacks from crop growth. Those feedbacks affect each of the evapotranspiration components in a specific manner.

We therefore model evapotranspiration as three separate and partly interdependent terms: crop transpiration, canopy interception evaporation, and soil evaporation. The parameters are calibrated using Feddes (1987).

As starting point, we used an adapted form of the dual crop coefficient approach given by Wright (1982) and Allen et al. (2005):

$$T_p + E_{s,p} = (K_{cb} + K_{ew}) ET_0 \quad (1)$$

where T_p is the potential crop transpiration (m d^{-1}), $E_{s,p}$ is the potential soil evaporation (m d^{-1}), K_{cb} is the basal crop coefficient, K_{ew} is the evaporation coefficient of a wet bare soil that is partly shielded by vegetation, and ET_0 is the reference crop evapotranspiration (m d^{-1}).

The reference crop evapotranspiration is calculated with the simplified Makkink equation, presented by De Bruin (1981, 1987):

$$ET_0 = 0.65 \frac{s}{s + \gamma} \frac{K^\downarrow}{L_v} c \quad (2)$$

where s is the slope of the vapour pressure curve, γ is the psychrometric constant ($\text{kPa } ^\circ\text{K}^{-1}$), K^\downarrow is the incoming global radiation (W m^{-2}), L_v is the latent heat of vaporization of water (J kg^{-1}), and c is a conversion factor ($\text{m d}^{-1} / \text{kg m}^{-2}\text{s}^{-1}$). De Bruin (1987) gives the following reasons for choosing the Makkink equation:

- a. Its behaviour is very similar to that of the Penman formula;
- b. It is remarkably simple: it requires only air temperature and global radiation as input,
- c. Under dry conditions Makkink’s formula performs better.

Soil evaporation also includes the evaporation from soil that is partly shielded by a canopy. The ‘bare’ soil is assumed to be ‘diffuse’, meaning that we do not distinguish between soil that is covered by vegetation and soil that is not. We assume that the net radiation inside the canopy decreases according to an exponential extinction function of the leaf area index (LAI) and that the soil heat flux can be neglected (Goudriaan, 1977; Belmans, 1983):

$$K_{ew} = e^{-\kappa_{gr} \text{LAI}} K_{ew100} \quad (3)$$

where κ_{gr} is the extinction coefficient for solar radiation (-), LAI the leaf area index, and K_{ew100} the evaporation coefficient of a wet soil receiving full radiation. Ritchie (1972) and Feddes (1978) used $\kappa_{gr} = 0.39$ for common crops. More recent approaches estimate κ_{gr} as the product of the dimensionless extinction coefficient for diffuse

visible light, κ_{df} , which varies with crop type from 0.4 to 1.1, and the extinction coefficient for direct visible light, κ_{dir} :

$$\kappa_{gr} = \kappa_{df} \kappa_{dr} \quad (4)$$

We use the method from Boesten and Stroosnijder (1986) to calculate actual soil evaporation. This method only requires the time sequence of rainfall events and the reference crop evapotranspiration multiplied by the K_{ew} coefficient; it has a proven track record in the Netherlands.

Soil moisture conditions are assumed to limit transpiration according to (Feddes et al., 1978):

$$T_a = \alpha_{rw} T_p \quad (5)$$

where T_a is the actual transpiration rate (m d^{-1}) and α_{rw} is a dimensionless stress coefficient [0-1] that gives the influence of available soil water on transpiration (Fig. 2).

A wet canopy leads to an increased evapotranspiration due to interception evaporation, which lowers resistance for the moisture flow from the canopy to the atmosphere. Wright (1982) accounts for this lower resistance by adjusting the crop and bare soil coefficients. We model these effects separately, via the mentioned soil evaporation method and by explicitly modelling canopy interception evaporation. Interception evaporation from a vegetation canopy is not sensitive to soil moisture conditions as described by the α_{rw} coefficient. This makes it relevant to model it separately from the transpiration.

To model canopy interception evaporation, Eq. (1) is expanded to:

$$T_p + E_{i,p} + E_{s,p} = (K_{cb} + K_{iw} + K_{ew}) ET_0 \quad (6)$$

where $E_{i,p}$ is the potential canopy evaporation rate, and K_{iw} is the evaporation coefficient of a wet canopy, with $K_{iw} > K_{cb}$. The actual canopy evaporation and dripping rate to the soil are determined with the method given by Rutter et al. (1971). It is adapted to account for the relative interception evaporation dependency on canopy storage. As Rutter remarks, a linear relationship entails that the complete drying out of a canopy takes an infinite time, which is not realistic. We have remedied this problem by assuming a discontinuous relationship with a ‘start-up’ value, instead of a linear one starting from zero, as described in Appendix A.

Evaporation from a wet canopy is assumed to be a dominant process: as long as it is active, the transpiration is assumed to be zero. This assumption is based on the notions that evaporation ‘has first choice’ for using the energy flux and that due to a higher air moisture content the transpiration is suppressed. To account for this dominance, the active time fraction W_{frac} is calculated:

$$W_{frac} = \frac{E_{i,a}}{E_{i,p}} \quad (7)$$

where $E_{i,a}$ is the actual canopy interception evaporation rate (m d^{-1}). This time fraction is used for expanding Eq. (5) to:

$$T_a = \alpha_{rw} T_p (1 - W_{frac})$$

2.5 Data summary

For the simulation period, the time series information of the meteorological conditions should be available in the form of a step-function with a time interval of t_s . That concerns both the precipitation and the data needed for simulating the evapotranspiration. For the Makkink method only the values of the reference evapotranspiration are needed. If the Penman-Monteith method is used the following data are needed:

- radiation;
- temperature;
- humidity;
- wind speed.

These data can be supplied for more than one gauging station in the region. In that case the relevant station should be specified for each of the SVAT-units of the soil water /groundwater model. A method for introducing extra spatial variation is to specify calibration factors for each of the SVAT's. It is also possible to specify all of the time-dependent data via 'grids' covering the spatial extent of the model area.

If the data are only available on a daily basis, then some form of downscaling should first be applied for simulating the interception evaporation with some degree of accuracy.

Per SVAT-unit the dominant land-use should be specified. The parameters of the transpiration reduction function are required for all methods, as are the light-extinction coefficients.

The time-dependent vegetation transpiration factor, the time-dependent interception evaporation factor and the time-dependent bare soil evaporation factor are only required for when the reference crop method is used; the ponding factor is always required. It is crucial that the factors supplied in a file are consistent with the chosen method for computing the reference crop evapotranspiration. For agricultural crops in combination with the Makkink reference evapotranspiration use can be made of the factors supplied by Feddes (1987)¹.

The time-dependent parameters of the interception reservoir should be always be given, for each type of vegetated land use.

The time-dependent crop height, the Albedo values and minimum canopy resistance are only needed if the Penman-Monteith method is used with crop-specific parameters. If it is used for the reference crop method the parameters are obtained from hard-wired values in the code.

¹ When interception is modelled separately the vegetation factors have to be transformed.

3 Soil water

3.1 Introduction

As indicated in the introductory chapter, water on the soil surface has a ‘multiple identity’. Here we describe the manner in which it takes part in the soil column processes, including the influence of atmospheric interactions described in the previous section. For the model formulation we use a ‘control box 0’ that extends upwards from the soil surface. The subsurface soil water dynamics are described using two control boxes: for the root zone, the shallow subsoil and the deep subsoil (Figure 6). We describe the unsaturated zone model in detail in §3.3. The water balances and simulations are made at the aggregate scale of the control boxes, but the model in fact has continuous moisture profiles ‘on the background’, meaning that at any desired moment the detailed head and moisture content profiles can be made available if needs be. This distinguishes the approach from models based on ‘lumping’ of the vertical domain.

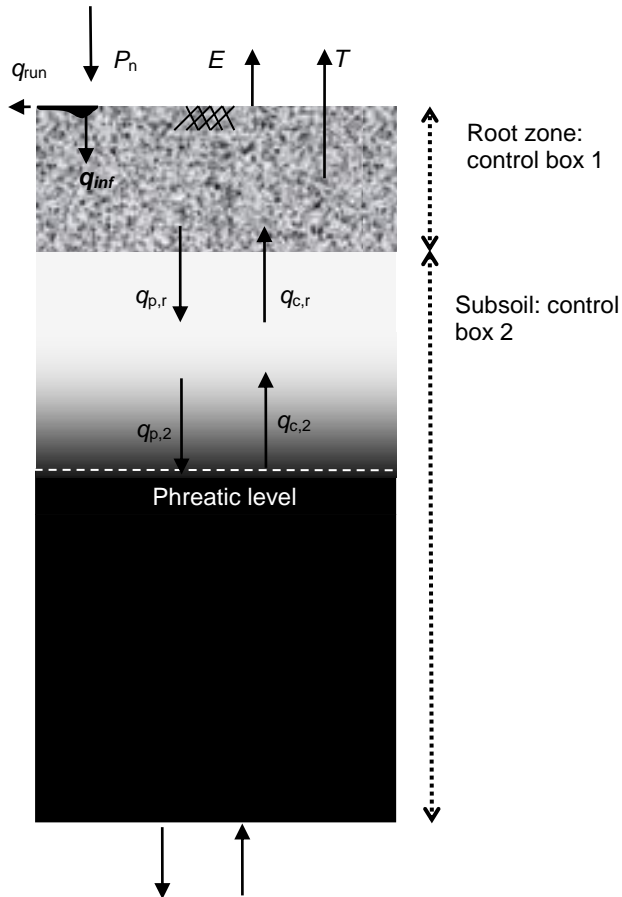


Figure 6 Flows in the soil water model. Explanation of symbols: P_n – net precipitation; q_{inf} – infiltration; q_{run} – surface runoff; E – evaporation of bare soil; T – transpiration; q_p – pervolution; q_c – capillary rise.

3.2 Ponding water and infiltration

3.2.1 Theory

Water stored on the soil surface has diverse functions and interactions. Here we confine ourselves to its role as a reservoir and as an intermediate source for supplying infiltration water. The storage on the soil surface is schematized into two fractions:

- ‘micro’-storage;
- ‘macro’-storage.

The microstorage is formed by small depressions in the soil surface at sub-grid scale. When after an inundation the land falls dry the water in the micro-storage is retained. The water in macro-storage can freely move over the soil surface, restricted only by natural barriers and constructions in the surface water channel network. The schematization of the surface water system can be extended to the soil surface, obtained from an GIS-analysis of the soil surface topography. In that case the barriers consist of the ‘saddle points’ in the soil surface landscape.

Ponding water that is ‘macro’-storage on the soil surface has a multiple identity. The steps involved in the multiple identity concept are described in §5.3.3 and illustrated in Figure 27 through Figure 31.

The modelling of infiltration is notoriously difficult for various reasons, of which we mention:

- the role of crust-forming at the soil surface;
- the complexity of the rewetting process of a dried out soil;
- the role of sub-grid scale flow processes over the soil surface; water that becomes runoff at one spot can after all infiltrate in a small depression just a few metres away.

We do not attempt to model these aspects via a formulation in terms of a differential equation. Instead we follow a pragmatic approach involving a minimum of parameters that still allow enough freedom for the modeller to control the simulation along broad lines.

The amount of water in the ponding reservoir (“ponding storage”) reacts directly to incoming precipitation and exchange with the surface water model; thus we model the dynamics of the ponding reservoir with the time step of the ‘fast’ processes. The use of a different time steps for the fast and slow processes can lead to numerical artefacts in the model if no precautions are taken. These precautions can take on two different forms:

- spreading of the effect of the *previous* update of the groundwater model on the new series of fast time steps;
- anticipation on the behaviour of the model during the *next* update of the groundwater model in reaction to fluxes and state variables of the fast processes.

3.2.2 Implementation

At the beginning of the first time cycle for the ‘fast’ processes within a new groundwater time step (see Figure 5) the groundwater above soil surface (if present) is converted into ponding water:

$$S_{\text{pond}}^{j=0} = \max\{0; h^{j=0} - h_{\text{ss}}\} \quad (3)$$

where:

$$\begin{aligned} S_{\text{pond}}^{j=0} &= \text{ponding storage at the beginning of the first ‘fast’ time cycle within the groundwater time step (m)} \\ h^{j=0} &= \text{groundwater level at time level } j=0 \text{ of the fast processes, i.e. at the end of the previous groundwater time step (m)} \\ h_{\text{ss}} &= \text{elevation of the soil surface (m)} \end{aligned}$$

The situation with upward seepage to the soil surface is handled in a special manner. The above equation is then implemented in a modified form, in which the influence of the upward seepage is spread out over *all* of the fast time steps within the considered groundwater time step. Without this modification the model would produce artificial peaks in the surface runoff during the first fast time step.

Infiltration can of course only occur if there is water available in the form of net precipitation and/or water stored from the preceding period. We give infiltration of ponding water priority over evaporation. So in order to determine the water availability for infiltration the amount of water in the ponding reservoir is first updated with:

$$S_{\text{pond}}'^{j+1} = S_{\text{pond}}^j + P_{\text{n}}^{\text{ave}} \Delta t_s \quad (4)$$

where:

$$\begin{aligned} S_{\text{pond}}^j &= \text{ponding storage at time level } j \text{ of fast processes (m)} \\ S_{\text{pond}}'^{j+1} &= \text{ponding storage after intermediate update for net precipitation (m)} \\ P_{\text{n}}^{\text{ave}} &= \text{net precipitation rate, time averaged (m d}^{-1}\text{)} \\ \Delta t_s &= \text{time step of fast time cycle (d)} \end{aligned}$$

The upper bound for the availability of infiltration water is then given by:

$$q_{\text{inf,max,pond}} = S_{\text{pond}}'^{j+1} / \Delta t_s \quad (5)$$

where $q_{\text{inf,max,pond}}$ is maximum available infiltration rate from ponding water (m d⁻¹)

For situations with free percolation to the groundwater we use a simple relationship for determining the maximum infiltration rate $q_{\text{inf,max}}$

$$q_{\text{inf,max}} = \min(q_{\text{inf,max,u}}, k_{\text{sat,l}}) + S_{\text{pond}}'^{j+1} / c_{\text{top,down}} \quad (6)$$

where:

$$q_{\text{inf,max}} = \text{maximum infiltration rate (m)}$$

$q_{\text{inf,max,u}}$	=	maximum infiltration rate for situations without ponding (m d ⁻¹)
$k_{\text{sat,l}}$	=	saturated conductivity of top layer of soil physical schematization (m d ⁻¹)
$c_{\text{top,down}}$	=	vertical flow resistance in top of soil (d)

The use of the term involving $c_{\text{top,down}}$ is optional. And the influence of the first term can be cancelled by specifying high values of the infiltration rate and of the saturated conductivity of the top layer.

In fully saturated conditions and with a specified $c_{\text{top,down}}$ the infiltration rate is found from the head difference between ponding water and groundwater divided by $c_{\text{top,down}}$. In situations with the head of the groundwater higher than that of the ponding water the resistance for upward flow is used $c_{\text{top,up}}$. If the resistance is not specified, then we assume freedom of movement of water through the soil surface in situations that are fully saturated.

Infiltration can also be hampered by a bottleneck further down in the system, i.e. in the soil water and/or groundwater system. Let us first consider the case with the groundwater level below the bottom of the root zone. The maximum amount of storage space available for infiltration is then estimated with:

$$S_{\text{inf,max,r}} = S_{\text{r,sat}} - S_{\text{r}}^{j=0} + (E_{\text{a}}^{\text{ave}} + T_{\text{a}}^{\text{ave}} - I^{\text{ave}} + q_{\text{p,max}}) \Delta t_{\text{g}} \quad (7)$$

$$q_{\text{inf,max,r}} = S_{\text{inf,max,r}} / \Delta t_{\text{s}}$$

where:

$S_{\text{inf,max,r}}$	=	available storage space for infiltration, based on root zone balance (m)
$S_{\text{r,sat}}$	=	saturated water content of root zone (m)
$S_{\text{r}}^{j=0}$	=	water content of root zone at the beginning of the first fast time cycle, i.e. the content at the end of the previous groundwater time step (m)
$E_{\text{a}}^{\text{ave}}$	=	soil evaporation of previous fast time steps, time-averaged over Δt_{g} (m d ⁻¹)
$T_{\text{a}}^{\text{ave}}$	=	transpiration of previous fast time steps, time-averaged over Δt_{g} (m d ⁻¹)
I^{ave}	=	infiltration during previous fast time steps, time averaged (m d ⁻¹)
$q_{\text{p,max}}$	=	maximum possible percolation rate (>0) to the groundwater (m d ⁻¹)
$q_{\text{inf,max,r}}$	=	maximum infiltration rate, based on root zone balance (m)
Δt_{g}	=	time step of soil water / groundwater submodels (d)

The above expression takes into account that evaporation and/or transpiration from the root zone makes storage space available for infiltration water. The values given in the above expression are still in the process of being updated, during each fast time cycle. The time-averaged values are used because it is the volume that determines the infiltration space. The maximum possible percolation rate to the groundwater is derived from the soil physical metafunction q_{m} given in §3.3.2.1.

The percolation can be hampered by the situation in the subsoil. For investigating this potential bottleneck a balance is made for the whole column:

$$\begin{aligned}
S_{\text{inf,max,c}} &= S_{\text{r,sat}} - S_{\text{r}}^{j=0} + S_{2,\text{sat}} - S_2^{j=0} + \\
&\quad (E_{\text{a}}^{\text{ave}} + T_{\text{a}}^{\text{ave}} - I^{\text{ave}} + Q_{\text{spgw}}^{\text{ave}} - Q_{\text{d}}^{\text{ave}} - G^{\text{ave}}) \Delta t_{\text{g}} \\
q_{\text{inf,max,c}} &= \max\{S_{\text{inf,max,c}} / \Delta t_{\text{s}}, 0\}
\end{aligned} \tag{8}$$

where:

$$\begin{aligned}
S_{\text{inf,max,c}} &= \text{maximum storage space for infiltration, based on column balance (m)} \\
S_{2,\text{sat}} &= \text{saturated water content of shallow subsoil (box 2) (m)} \\
S_2^{j=0} &= \text{water content of root zone at the beginning of first fast time cycle (m)} \\
Q_{\text{spgw}}^{\text{ave}} &= \text{extraction for sprinkling from groundwater (from first layer) (m d}^{-1}\text{)} \\
Q_{\text{d}}^{\text{ave}} &= \text{drainage / infiltration (+ = to the column) (m d}^{-1}\text{)} \\
G^{\text{ave}} &= \text{regional groundwater flow (+ = to the column) , last known value (m d}^{-1}\text{)} \\
q_{\text{inf,max,c}} &= \text{maximum infiltration rate, based on column balance (m)}
\end{aligned}$$

The infiltration is then found from:

$$q_{\text{inf}} = \min(q_{\text{inf,max,pond}}; q_{\text{inf,max,u}}; q_{\text{inf,max,r}}; q_{\text{inf,max,c}}) \tag{9}$$

The next update of the water stored in the ponding reservoir is made with:

$$S_{\text{pond}}^{j+1} = S_{\text{pond}}^{j+1} - q_{\text{inf}} \Delta t_{\text{s}} \tag{10}$$

where:

$$S_{\text{pond}}^{j+1} = \text{ponding storage water after update for infiltration (m)}$$

The value of S_{pond}^{j+1} is used for determining the maximum availability of ponding evaporation water (Eq. **Error! Reference source not found.**). Subsequently the amount of ater in storage is updated with:

$$S_{\text{pond}}^{j+1} = S_{\text{pond}}^{j+1} - E_{\text{pond}} \Delta t_{\text{s}} \tag{11}$$

where:

$$\begin{aligned}
S_{\text{pond}}^{j+1} &= \text{ponding storage after update for evaporation (m)} \\
E_{\text{pond}} &= \text{ponding evaporation rate (m d}^{-1}\text{)}
\end{aligned}$$

The way the runoff is computed depends on the used modelling option:

- the resistance method;
- the integrated method involving zero resistance.

The advantage of the first method is that the time-delay due to the flow process is modelled to some extent. The disadvantage is that due to the low resistance the simulation can become unstable, and oscillations result. The integrated method is unconditionally stable; the drawback is the immediacy of transfer of water, which can be unrealistic.

If the resistance method is used the runoff is simply computed with:

$$q_{\text{run}} = [h_s^j - S_{\text{pond}}^{j+1}] / \Delta t_s \quad (12)$$

where:

$$\begin{aligned} q_{\text{run}} &= \text{runon/runoff of the SVAT-unit (+ = to the column) (m d}^{-1}\text{)} \\ h_s^j &= \text{surface water level at time level } j \text{ (m)} \end{aligned}$$

If the integrated method used for the runoff simulation (see §5.3.3 and Figure 27 through Figure 31), the ponding water in the *macro*-storage is transferred to the surface water model. For this the storage is first decomposed into the two types of storage with:

$$\begin{aligned} S_{\text{pondmicro}}^{j+1} &= \min\{S_{\text{pond}}^{j+1}; S_{\text{pondmicro, cap}}\} \\ S_{\text{pondmacro}}^{j+1} &= S_{\text{pond}}^{j+1} - S_{\text{pondmicro}}^{j+1} \end{aligned} \quad (13)$$

where:

$$\begin{aligned} S_{\text{pondmicro}}^{j+1} &= \text{ponding micro-storage (m)} \\ S_{\text{pondmicro, cap}} &= \text{capacity of micro-storage (m)} \\ S_{\text{pondmacro}}^{j+1} &= \text{ponding macro-storage (m)} \end{aligned}$$

The surface water model then computes hydraulic heads for the channel trajectories and the associated subcatchments; each subcatchment consists of one or more SVAT-units of the top system model. After completing the simulation of surface water flow processes the newly determined levels are linked to the respective SVAT-units within the subcatchments. The modified amount of water in macro-storage is computed by:

$$S_{\text{pondmacro}}^{j+1} = \max\{h_s - (h_{ss} + S_{\text{pondmicro, cap}}); 0\} \quad (14)$$

where:

$$\begin{aligned} S_{\text{pondmacro}}^{j+1} &= \text{ponding water in macro-storage after surface water update (m)} \\ h_s &= \text{surface water level (m)} \\ h_{ss} &= \text{elevation of the soil surface (m)} \end{aligned}$$

and the total storage in the ponding reservoir is computed as

$$S_{\text{pond}}^{j+1} = S_{\text{pondmicro}}^{j+1} + S_{\text{pondmacro}}^{j+1} \quad (15)$$

where:

$$S_{\text{pond}}^{j+1} = \text{ponding water after update for surface water flow (m)}$$

By comparing this storage to the amount that was transferred to the surface water model, the net runon/runoff of the SVAT-unit can be calculated (>0 for runon):

$$q_{\text{run}} = [S_{\text{pond}}^{j+1} - S_{\text{pond}}^{j+1}] / \Delta t_s \quad (16)$$

where:

$$q_{\text{run}} = \text{runon/runoff of the SVAT-unit (m d}^{-1}\text{)}$$

If the considered ‘fast’ time step involves an intermediate update within the (longer) groundwater time step, the final ponding storage S_{pond}^{j+1} is set equal to $S_{\text{pond}}^{\prime\prime\prime j+1}$. The simulation then continues with the next cycle starting from Eq. 4. If the simulation has arrived at the end of the last ‘fast’ time cycle it is followed by a finalization procedure. In the case that there is hydraulic contact with the groundwater the ponding storage is compared to that at the beginning. The difference is added as recharge to the groundwater model:

$$q_{\text{recha,pond}} = (S_{\text{pond}}^{\prime\prime\prime j=n} - S_{\text{pond}}^{j=0}) / \Delta t_g \quad (17)$$

where:

$$\begin{aligned} q_{\text{recha,pond}} &= \text{recharge rate of the ‘visible’ groundwater, time averaged over } \Delta t_g \text{ (m)} \\ S_{\text{pond}}^{j=0} &= \text{ponding storage at beginning of groundwater time step (m)} \\ S_{\text{pond}}^{\prime\prime\prime j=n} &= \text{ponding storage at end of last ‘fast’ time step } n, n = \Delta t_g / \Delta t_s \text{ (m)} \end{aligned}$$

After the groundwater model update has been performed, the ponding storage $S_{\text{pond}}^{j=n}$ is finalized by applying Eq. 3 for the new groundwater level. At this point the infiltration rate can also be finalized on the basis of a water balance analysis involving the final value of G^{ave} , the regional groundwater flow.

3.3 Unsaturated flow

3.3.1 Theory

The model schematization assumes that unsaturated flow takes place within parallel vertical columns, with each column connecting to a simulation unit of a groundwater model. The phreatic surface acts as a ‘moving boundary’ between the flow domains of the soil column models and the groundwater model. All lateral exchanges are assumed to take place in the saturated zone. The main idea of the modeling method for the (unsteady) unsaturated flow is to use steady-state solutions to Richards’ equation as building blocks of a dynamic model, a so-called quasi steady-state model. The appropriate building blocks are – for each time level – selected on the basis of water balances at the aggregate scale of control volumes for the ‘root zone’ and the ‘subsoil’. Put in mathematical terms, the partial differential equation for the unsteady flow (Richards’ equation) is replaced by two ordinary differential equations: one for the variations in the vertical column (using the steady-state form of the flow equation) and the other for the variations in time (using a water balance at aggregate scale). The described method is a radical redesign of the one presented by de Laat (1980) and Wesseling (1957). A validation of the current method is given in Van Walsum and Groenendijk (2008).

3.3.1.1 Steady states

For one-dimensional flow in an unsaturated soil with root water extraction, the steady-state form of the flow equation can be written as:

$$\frac{d}{dz} \left[K(\psi) \left(\frac{d\psi}{dz} + 1 \right) \right] - \tau(\psi, z) = 0, \quad 0 \geq z \geq b, \quad (18)$$

subject to the boundary conditions

$$\psi(b) = 0 \quad (19)$$

$$\left[K(\psi) \left(\frac{d\psi}{dz} + 1 \right) \right]_{z=0} = -q(0) \quad (20)$$

where

z	=	elevation coordinate, taken positively upward (zero at the soil surface) (m)
b	=	groundwater elevation (m)
ψ	=	pressure head (m)
$K(\psi)$	=	hydraulic conductivity as a function of pressure head (m d ⁻¹)
$q(0)$	=	flux density at the soil surface, taken positively upward (m d ⁻¹)
$\tau(\psi, z)$	=	depth- and head-dependent extraction term for root water uptake (m ³ m ⁻³ d ⁻¹)

A steady-state profile is obtained by specifying the conductivity parameters of each distinguished soil layer and by solving Eq. 18 subject to imposed values for the groundwater elevation b (Eq. 19), the *potential* flux density at the soil surface $q_{\text{pot}}(0)$ (Eq. 20), and the *potential* total root water uptake rate T_{pot} of the root zone. A flexible root

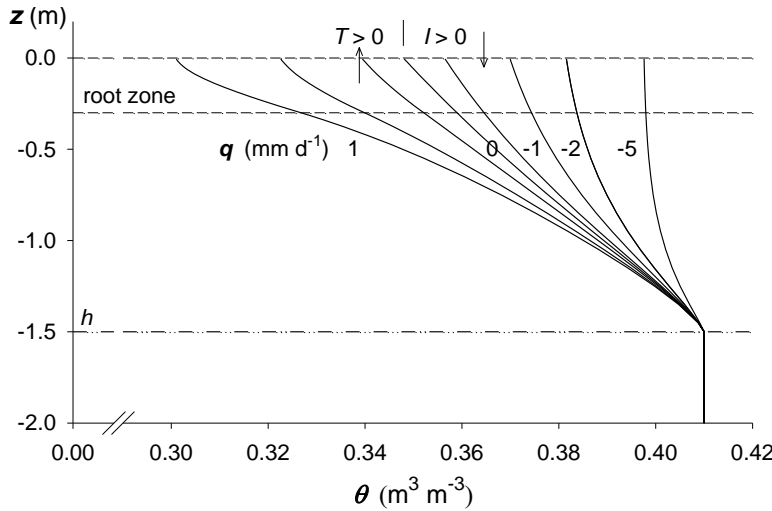


Figure 7 Examples of steady-state profiles for a loamy soil with a root zone thickness of 0.3 m and a groundwater elevation of -1.5 m. For the capillary rise profiles (transpiration rate $T > 0$) the given values of the flux density ($q > 0$) are for below the root zone; for the equilibrium profile and the percolation profiles (infiltration rate $I \geq 0$) the given values of the flux density ($q \leq 0$) are for the whole profile down to the groundwater elevation. The Mualem-Van Genuchten parameters (Mualem, 1976; Van Genuchten, 1980) given by Wösten *et al.* (2001) for this homogeneous soil are $\theta_s = 0.41 \text{ m}^3 \text{ m}^{-3}$, $\theta_r = 0.01 \text{ m}^3 \text{ m}^{-3}$, $k_s = 0.0370 \text{ m d}^{-1}$, $a = 0.71 \text{ m}^{-1}$, $n = 1.298$, $\lambda = 0.912$.

distribution function with depth is applied, yielding the potential root extraction rate $\tau_{\text{pot}}(z)$. The actual root extraction rate is obtained (as part of the solution scheme for Eq. 18) through multiplying the potential extraction rate by a dimensionless reduction function (Feddes *et al.*, 1978). The solution obtained by running a steady-state version of the SWAP model (Appendix 1, see also Kroes *et al.*, 2008) yields values for the *actual* root extraction rate $\tau_{\text{act}}(z)$, the *actual* flux density $q(0)$ at the soil surface, and the constant moisture flux density q in the subsoil below the root zone. The flow in the saturated part of the profile is outside the domain of the steady-state simulations. Examples of steady-state profiles for a root zone thickness of 0.3 m and a groundwater elevation $h = -1.5$ m are given in Figure 7.

The set of steady-state profiles which result from different combinations of groundwater elevation, potential flux density at the soil surface $q_{\text{pot}}(0)$, and potential total root water uptake T_{pot} , is assumed to be available in a database. For the sake of simplicity, the database only contains steady states resulting from either a non-zero $q_{\text{pot}}(0) < 0$ or a non-zero $T_{\text{pot}} > 0$, plus the equilibrium profiles. From the states contained in the database, it is then possible to construct a function $\Psi(z, q, h)$ for the pressure head (m) as a function of the elevation z (m), the steady-state flux density q below the root zone (m d^{-1}), and the groundwater elevation h (m). Combining $\Psi(z, q, h)$ with a relationship between moisture content and pressure head (Van Genuchten, 1980) yields the function $\Theta(z, q, h)$ for the volumetric water content ($\text{m}^3 \text{ m}^{-3}$) as a function of z , q , and h .

In utilizing the profiles, frequent reference is made to a profile ‘segment’. By a ‘root zone profile segment’ is meant the part of a profile for $z \geq z_r$, where z_r is the elevation of the bottom of the root zone. By a ‘subsoil segment’ is meant the part of a profile for $z < z_r$, extending downwards to an elevation z_s (which is taken below the deepest groundwater elevation that can locally occur). Water content totals of the profile segments are obtained through integration:

$$s_r = \int_{z_r}^0 \theta(z) dz; \quad s_s = \int_{z_s}^{z_r} \theta(z) dz; \quad s = \int_{z_s}^0 \theta(z) dz \quad (21)$$

where:

- $\theta(\mathcal{Z})$ = volumetric water content at elevation \mathcal{Z} ($\text{m}^3 \text{m}^{-3}$)
- s_r = total water content of the root zone (m)
- s_s = total water content of the ‘subsoil’ (m)
- s = total of s_r and s_s (m).

3.3.3.2 Dynamics

Recharge

Flow dynamics are driven by time variations of water balance stresses in the root zone. These stresses are summarized by the root zone recharge rate:

$$R = I - E - \int_{\mathcal{Z}_r}^0 \tau_{\text{act}}(\mathcal{Z}) d\mathcal{Z} \quad (22)$$

where:

- R = root zone recharge rate (m d^{-1})
- I = infiltration rate at the soil surface (m d^{-1})
- E = soil evaporation rate (m d^{-1})
- $\tau_{\text{act}}(\mathcal{Z})$ = actual root extraction rate as a function of \mathcal{Z} ($\text{m}^3 \text{m}^{-3} \text{d}^{-1}$)

The head-dependent function for root extraction is nonlinear (Feddes *et al.*, 1978); it is therefore important for the accuracy to evaluate the dependency at a detailed scale in the vertical column. The use of a total recharge rate implies that infiltration at the soil surface is assumed to be distributed instantaneously throughout the root zone according to one of the steady-state water content profiles. It is part of the solution procedure to determine which profile that is.

Transitions between steady states

In solving the equations describing the soil water dynamics, use is made of the following properties of the $\Theta(\mathcal{Z}, q, h)$ function:

1. For a given groundwater elevation, the total amount of water s in a steady-state profile is a strictly monotonously *decreasing* function of the steady-state flux q (taken positively upward). The same applies to the total amount of water present in the profile from the groundwater elevation upwards.
2. For a given moisture content at the top of the profile, the total amount of water in the profile is a strictly monotonously *increasing* function of the groundwater elevation h .

To describe the method, first two hypothetical cases of a drying-out soil are considered. Both start from a steady-state moisture profile involving root zone extraction (meaning a negative recharge rate R) and capillary rise. The cases differ with respect to the boundary conditions starting from time t^j , where the superscript j denotes the time level.

In Case 1 (Figure 8) the extraction suddenly increases to a new value T^{j+1} that is assumed to be known; the groundwater elevation is held constant by supplying sufficient lateral saturated flow to compensate for the capillary rise. The schematization of the quasi steady-state method entails that the water content profile at t^{j+1} has to be found by selecting one of the profiles from the database of steady states. The unknown to be solved is the (new) steady-state flux density at t^{j+1} : If that flux density is known, then (in

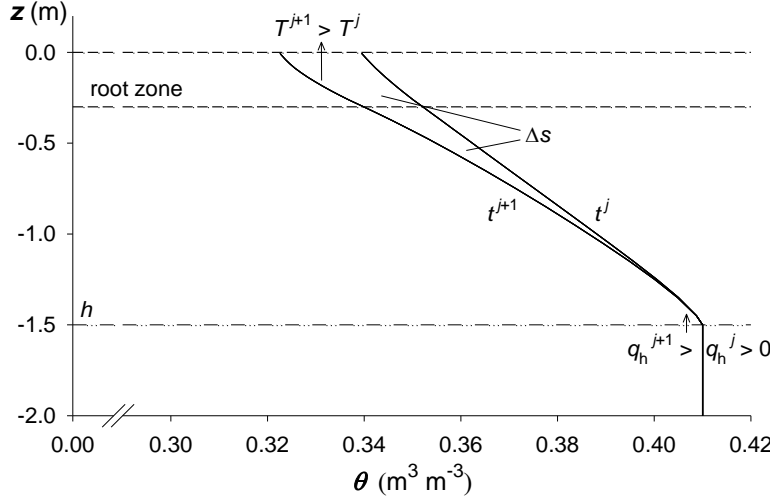


Figure 8 Case 1 of a drying-out soil: Increasing extraction from the root zone ($T^{j+1} > T^j$) and the groundwater elevation h held constant. The simulated transition from the steady-state profile at time t^j to a steady-state profile at t^{j+1} is based on a water balance at aggregate scale, using the time-averaged transpiration rate T^{ave} , the total volume change Δs , and the time-averaged flux density q_h^{ave} from the phreatic surface.

combination with the known groundwater elevation h) the rest of the profile is known. The solution is found by formulating a water balance equation for the vadose zone as a system volume, assuming that the value of q in the $\Theta(z, q, h)$ function occurs at the phreatic surface:

$$\int_b^0 [\theta^{j+1}(z) - \theta^j(z)] dz - q_h^{ave} \Delta t_g = R^{ave} \Delta t_g \quad (23)$$

$$\theta^{j+1}(z) = \Theta(z, q_h^{j+1}, h)$$

where:

- R^{ave} = time-averaged recharge rate (which in Case 1 is equal to $-T^{j+1}$) (m d^{-1})
- q_h^{j+1} = flux density through the phreatic surface at time t^{j+1} (m d^{-1})
- q_h^{ave} = time-averaged flux density during the interval $[t^j, t^{j+1}]$ (m d^{-1})
- Δt_g = time increment $[t^{j+1} - t^j]$ (d)

The time-averaged flux density is computed with a weighting factor $f(-)$ for the time dependence:

$$q_h^{ave} = (1-f)q_h^j + f q_h^{j+1} \quad (24)$$

Then, after rearranging, Eq. 23a can be written as:

$$\int_b^0 \theta^{j+1}(z) dz - f q_h^{j+1} \Delta t = \int_b^0 \theta^j(z) dz + (1-f) q_h^j \Delta t + R^{ave} \Delta t \quad (25)$$

From property 1 of the set of steady states it follows that the left side of Eq. 25 (in combination with Eq. 23b) is a strictly monotonously decreasing function of the steady-state flux at t^{j+1} . For a given value of the right side of Eq. 25, it is possible to scan the set of steady states and then find the (only) one that satisfies the equation. This yields the

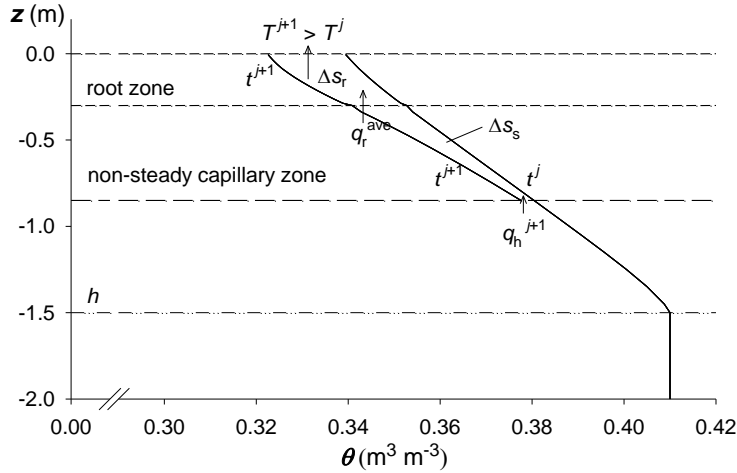


Figure 9 Use of a so-called composite profile in the alternative solution method for situations with capillary rise and deep groundwater elevations, applied to the hypothetical Case 1 of a drying-out soil (cf. Figure 8). In the first step of the solution procedure, a water balance is made for combined root zone and non-steady capillary zone (with $\Delta s_r + \Delta s_s$ as the total volume change) to obtain the profile segment at t^{j+1} , yielding also the time-averaged flux through the bottom of the root zone, q_r^{ave} . The profile segment between the bottom of the non-steady capillary zone and the groundwater level is assumed to not dry out beyond equilibrium profile.

unknown q_h^{j+1} and thereby (in combination with h) the whole water content profile by inserting the values in the $\Theta(z, q, h)$ function.

The above method assumes a transition of the whole profile to a new steady state. This, however, is only realistic for very shallow groundwater levels. For a drying-out soil, it is more realistic to let the water content profile in the subsoil lag behind that of the root zone. The 'cut' where the lag starts (Figure 9) is not taken at the bottom of the root zone, because below the root zone there is what we call the 'non-steady capillary zone' that is strongly influenced by the root water uptake activity. The thickness of this zone depends on the combined conductivity and storage characteristics of a soil. This thickness has to be found by calibration of the water balance on the SWAP model. For the profile segment towards the groundwater level we assume that it only acts as a transmission

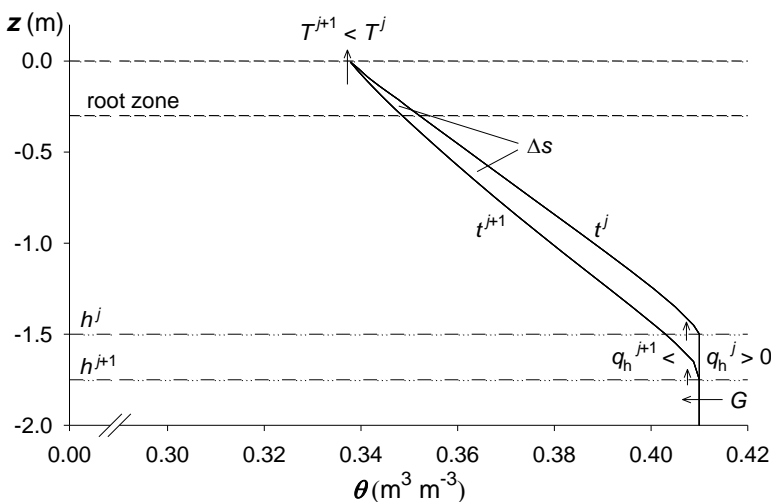


Figure 10 Case 2 of a drying-out soil: Moisture content at the top of the profile held constant and a falling groundwater elevation due to capillary rise. A water balance involving the time-averaged transpiration rate T^{ave} , the total volume change Δs , and the saturated flow to the soil column G is used for simulating the transition to a groundwater elevation h^{j+1} , assuming that the water content profile at t^{j+1} is a steady state profile.

zone for capillary fluxes that are determined by the situation in the root zone and the depth of the groundwater level.

In the (hypothetical) Case 2 (Figure 10) the moisture content at the top of the profile is kept constant. That is done by slowly reducing the extraction. This compensates for the decrease of capillary rise due to the falling groundwater elevation. The lateral saturated flow is assumed to be zero. In this (hypothetical) case the extraction rate as a function of time is assumed to be known. The unknown to be solved is the groundwater elevation as a function of time. That is done by formulating a water balance condition for a control volume of the soil column extending into the groundwater:

$$\int_{z_s}^0 [\theta^{j+1}(z) - \theta^j(z)] dz = [R^{ave} + G^{ave}] \Delta t$$

$$\theta^{j+1}(z) = \Theta(z, q^{j+1}, h^{j+1}) \quad (26)$$

$$\theta^{j+1}(0) = \theta^j(0)$$

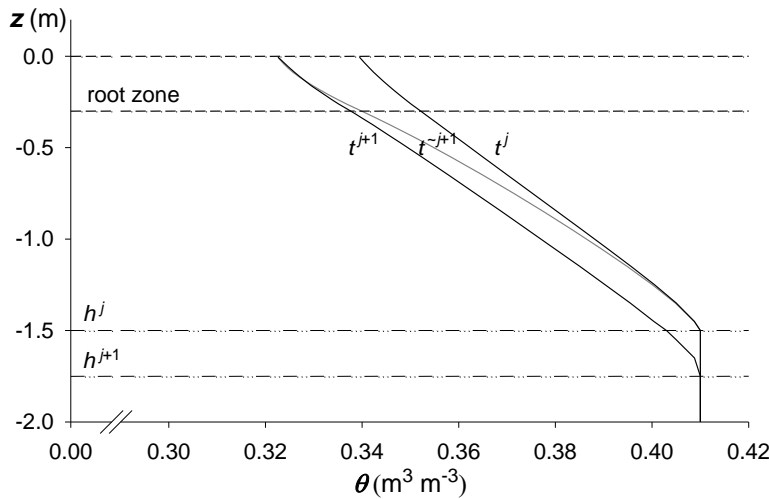


Figure 11 General case of a drying-out soil, involving both a water content change at the top of the profile and a groundwater elevation change: The moisture profile at $t = t^{j+1}$ is used for 'partitioning' the water content change from t^j to t^{j+1} . The profile at $t^{~j+1}$ is denoted as the 'intermediate update'

where the saturated flow G to the soil column (m d^{-1}) is assumed to be zero in this hypothetical case. This equation uniquely determines the groundwater elevation at t^{j+1} , owing to property 2 of the set of steady states: Eq. 26a can be rearranged like was done with Eq. 23a, resulting in an equation with the unknown θ^{j+1} on the left side. The solution at t^{j+1} is then found by scanning the subset of steady-states that complies with Eqs. 26b and 26c, and finding the (only) one that satisfies the rearranged form of Eq. 26a.

The general case (Figure 11) involves both a groundwater elevation change and a change in the water content at the top of the profile. In order to find a unique solution in a straightforward manner, the transition of the profile from t^j to t^{j+1} is partitioned. This is done with the moisture profile for the groundwater elevation at t^j and the moisture content at the top of the profile at t^{j+1} , as indicated in Figure 11 by the curve at $t^{~j+1}$. The partitioning of the water-content change is based on the notion that the recharge of the root zone acts as a driver of the processes in the column; thus the groundwater elevation

change is a *reaction to* what happens above. Furthermore, this way of partitioning greatly simplifies the solution method, which then can consist of two major steps that are performed consecutively:

1. for the unchanged groundwater elevation, determine the intermediate update at t^{j+1} ;
2. for the new moisture conditions in the top part of the profile, determine the new groundwater elevation at t^{j+1} .

The used solution method for the step 1 is the same as for the hypothetical Case 1 described above. In this step the elevation of the phreatic surface is assumed unchanged; thus the elevation is used in an ‘explicit’ manner with respect to time. The method for step 2 deviates from the method for Case 2 only in the handling of the moisture conditions in the top part of the profile, as is explained in the section about the model implementation.

For simulating situations with percolation, the first ‘cut’ of the profile is assumed to be at the bottom of the root zone. A separate calculation is made for the non-steady capillary zone and for the zones below. These extra zones form a cascade of profile segments, that simulate attenuation and transmission processes of soil moisture flow to deep groundwater levels.

3.3.3.3 Flux density profile

The flux density profile can be made explicit through making a water balance for each desired elevation coordinate z_i :

$$q^{ave}(z_i) = G^{ave} - \int_{z_s}^{z_i} \{[\theta^{j+1}(z) - \theta^j(z)] / \Delta t_g + \tau_{act}^{ave}(z)\} dz \quad (27)$$

where:

$$\begin{aligned} q^{ave}(z_i) &= \text{time-averaged flux density (m d}^{-1}\text{)} \\ G^{ave} &= \text{time-averaged saturated flow to the column (m d}^{-1}\text{)}, \\ \tau_{act}^{ave}(z) &= \text{time-averaged actual root extraction rate (m}^3\text{ m}^{-3}\text{ d}^{-1}\text{)} \end{aligned}$$

The term involving θ is the so-called *volume change rate*. This causes the time-averaged ‘quasi steady-state’ flux densities to differ from the steady-state flux density of a steady-state water content profile. The computed fluxes for elevations below the phreatic surface are outside the flow domain of the soil column model. For accurate simulation of water quality processes, they should be replaced by fluxes that are determined in the groundwater model.

3.3.2 Implementation

For the method to be efficient, it is crucial that the computational effort for running a regional hydrologic model (describing three dimensional groundwater flow coupled to the one-dimensional flow in the unsaturated zone) should be kept to a minimum. To that end, the numerics are done insofar as possible in the pre- and post-processing stages.

3.3.2.1 Pre-processing

In the pre-processing stage, a series of steady states for each soil type and possible root zone depth are computed using the numerical scheme given in Appendix 1. The simulations are done for the following boundary conditions:

- a series of (potential) boundary flux values for the root zone, ranging from extreme potential infiltration to extreme potential evapotranspiration;
- a series of groundwater elevations, ranging from just below the soil surface to the deepest depth present in the study region.

The used soil type definitions may involve several soil layers having different hydraulic properties. For each of the computed steady-state profiles, the mean pressure head in the root zone is determined with:

$$\psi_r = \frac{1}{|z_r|} \int_{z_r}^0 \psi(z) dz \quad (28)$$

where:

- z_r = elevation of the bottom of the root zone (m)
- $\psi(z)$ = pressure head as a function of z in one of the steady-state profiles (m d⁻¹).

Each steady-state profile has a unique combination of ψ_r and groundwater elevation h . These two variables serve as entries in tabular functions. This deviates from the use of the flux density q as an ‘independent’ variable in the functions $\Theta(z, q, h)$ and $\Psi(z, q, h)$ that are employed in describing the method. In the implementation of the model the flux density is handled as a *tabular function*, $\mathbf{TB}q(\psi_r, h)$. Using ψ_r instead of q as an independent variable appears to be more convenient for the algorithmic part of the implementation. The function $\Psi(z, q, h)$ for the pressure head is implemented as the set of tabular functions $\mathbf{TB}\Psi_i(\psi_r, h)$, for all compartments i of the Richards-type model used in the pre-processing. The function $\Theta(z, q, h)$ for the water content is implemented as $\mathbf{TB}\Theta_i(\psi_r, h)$, and also at the aggregate scale of the used *control volumes*, using the integrations given in Eq. 21:

- $\mathbf{TB}s_r(\psi_r, h)$ for the total storage of water in the root zone (m);
- $\mathbf{TB}s_s(\psi_r, h)$ for the total storage of water in the subsoil (m).

Examples of a storage and of a flux-density function are given in Figure 12 and Figure 13. (Note that the pF-axes of the two figures are different, for graphical reasons.) The steady-state simulations only yield values for physically possible combinations of ψ_r and h . So there is only partial independence of these two variables. In order to make possible a step-by-step solution procedure, the functions are extended to the whole domain of ψ_r and h , simply based on the rule ‘groundwater prevails’.

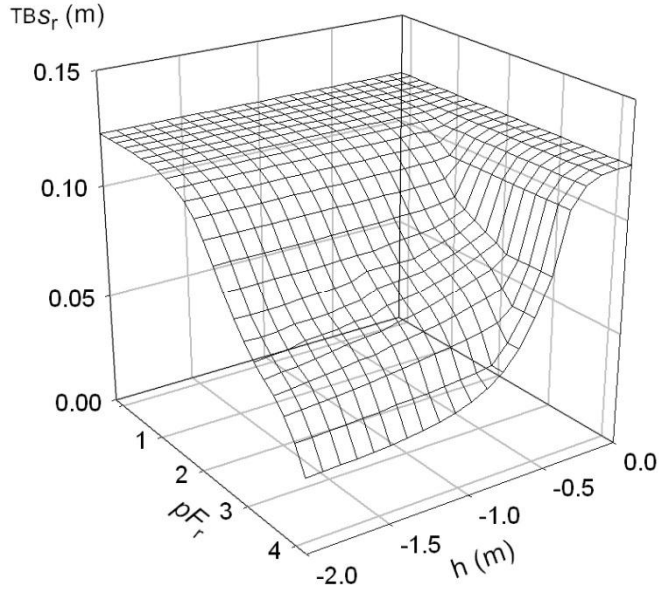


Figure 12 Example of a tabular root zone storage function $\mathbf{TBS}_r(\psi_r, h)$ for a loamy soil with a root zone thickness of 0.30 m. (For soil type 21 of Table 2; the parameters are given in the caption of Figure 7.) The total storage in the root zone is a function of the mean pressure head in the root zone (p^F of ψ_r) and the groundwater elevation (h).

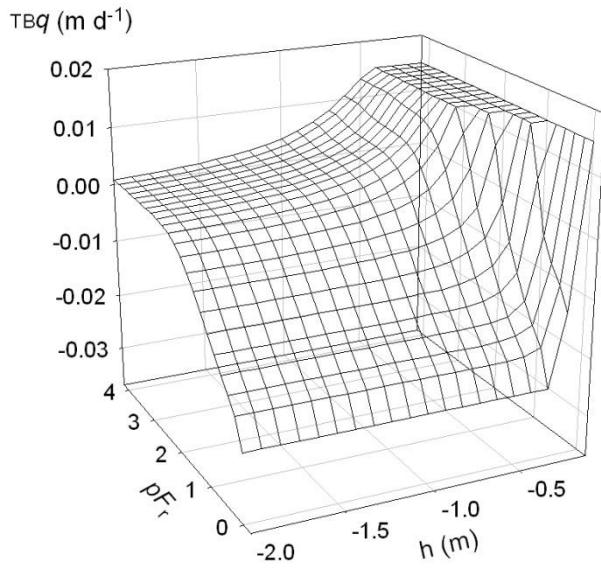


Figure 13 Example of a tabular moisture flux density function $\mathbf{TBq}(\psi_r, h)$ for a loamy soil with a root zone thickness of 0.30 m. (For soil type 21 of Table 2.) The steady-state flux density is given as a function of the mean pressure head in the root zone (p^F of ψ_r) and the groundwater elevation (h).

3.3.2.2 Online computational scheme

Overview

The ‘online’ part of the calculations is done in combination with a regional hydrologic model, with feedback at each time step; the scheme involves three major steps:

1. calculation of the recharge of the root zone;
2. update of the root zone pressure heads of the moisture profile segments (step 2a for the root zone update and step 2b for the subsoil update), yielding the values for the intermediate solution step at t^{j+1} ;
3. update of the groundwater elevation in conjunction with a groundwater model; finalization of root zone pressure heads, yielding the values at t^{j+1} .

Since an explicit scheme is employed for handling some of the variables with respect to time, the accuracy of the method is sensitive to the time increment used. Step 3 contains special precautions to ensure the stability of the scheme. A numerical example is employed for explaining the computational steps. For the example, we use the soil with a root zone thickness of 0.30 m that was previously drawn on in the illustrations. The initial groundwater elevation h at time t^j is -1.5 m and the moisture profile in the vadose zone is at equilibrium. A time step of 1 d is used. The third step of the scheme is described in Section §3.4.

Recharge

The recharge of the root zone (step 1) is computed as the net balance of the following three components: infiltration at the soil surface, evaporation, and root extraction (Eq. 22). The mean pressure head of the root zone is disaggregated to a more detailed level of compartments i (which are also used in solving the steady-state form of Richards’ equation) by evaluating the functions $\mathbf{TB}\Psi_i(\psi_i, h)$; then more accurate results are obtained for the total root water uptake. The time-averaged recharge rate is set equal to the value that is obtained using state variables (ψ_i) at the beginning of the time step; so an ‘explicit’ scheme is used. In the numerical example, there is a recharge rate of $R^{\text{ave}} = I^{\text{ave}} = 0.016 \text{ m d}^{-1}$ for the time step from t^j to t^{j+1} .

Root zone pressure head

In step 2a of the solution scheme, ψ_r (the mean pressure head of the root zone) is updated. This yields the value for the intermediate solution step, ψ_r^{j+1} . In the initial situation the equilibrium pressure head varies from -1.5 m at the soil surface to -1.2 m at the bottom of the root zone; so the mean value is equal to -1.35 m, which corresponds to a pF-value of 2.13. For this value in combination with $h = -1.5$ m, the tabular function displayed in Figure 12 gives a total storage in the root zone of $s_r^j = 0.1058$ m. According to the model concept, the infiltration water (0.016 m) will be spread throughout the root zone; so it is certain that the model will simulate percolation from the root zone during this time interval. In that case a variation of the solution method is used, involving separate profile segments for the root zone and the subsoil. A fully implicit scheme for the time weighting of the moisture flux is employed in this example; so $q_r^{\text{ave}} = q_r^{j+1}$. The balance is obtained in the following form:

$$\int_{\tilde{z}_r}^0 \theta^{j+1}(\tilde{z}) dz - q_r^{j+1} \Delta t_g = \int_{\tilde{z}_r}^0 \theta^j(\tilde{z}) dz + R^{\text{ave}} \Delta t_g = s_r^j + R^{\text{ave}} \Delta t_g = 0.1058 + 0.0160 = 0.1218 \text{ m} \quad (29)$$

The terms on the left side are now replaced by the respective tabular functions, with the unknown root zone pressure head ψ_r^{j+1} as one of the arguments:

$$\text{TB } s_r(\psi_r^{\sim j+1}, b^j) - \text{TB } q(\psi_r^{\sim j+1}, b^j) \Delta t_g = 0.1218 \text{ m} \quad (30)$$

The groundwater elevation is assumed unchanged in the intermediate solution step for the pressure heads; so b^j is used. This equation can be solved directly for $\psi_r^{\sim j+1}$ by first constructing a table for the total of the left side; the solution method is similar to the one used by Veldhuizen *et al.* (1998) in a simplified surface water model. The table can be interpreted as a ‘water demand’ function: the left side of Eq. 30 gives the total amount of water needed for storage and percolation, in dependence on $\psi_r^{\sim j+1}$. The demand must be matched to the ‘water availability’, which is 0.1218 m in the example. As can be derived from Table 1 through an inverse interpolation, a value of 0.1218 m for the availability matches to $\text{pF}_r^{\sim j+1} = 1.62$ ($=1.80 + \{[0.1218 - 0.1169]/[0.1222 - 0.1169]\} * [1.60 - 1.80]$), and thus $\psi_r^{\sim j+1} = -0.41$ m. This procedure also yields $s_r^{\sim j+1} = 0.1180$ m and $q_r^{\text{ave}} = q_r^{\sim j+1} = -0.0038 \text{ m d}^{-1}$.

After the update of the root zone variables, the flux to the subsoil is available for making the balance of the subsoil. Thereafter, a similar process of matching water availability and water demand serves as the solution procedure for the pressure head of the subsoil segment. Only the result is mentioned here. Assuming the bottom of the subsoil control volume is at $z_s = -2.0$ m, then the initial storage s_s^j in the subsoil equals 0.6668 m. The result for the intermediate update (Figure 14) is a storage of $s_s^{\sim j+1} = 0.6702$, which implies a change of $\Delta s_s^{\sim j+1} = 0.0034$ m and a time-averaged flux to the phreatic surface of $[-q_h^{\text{ave}}] = 0.0004 \text{ m d}^{-1}$. The new total storage in the column is given by $s^{\sim j+1} = s_r^{\sim j+1} + s_s^{\sim j+1} = 0.1180 + 0.6702 = 0.7882$ m.

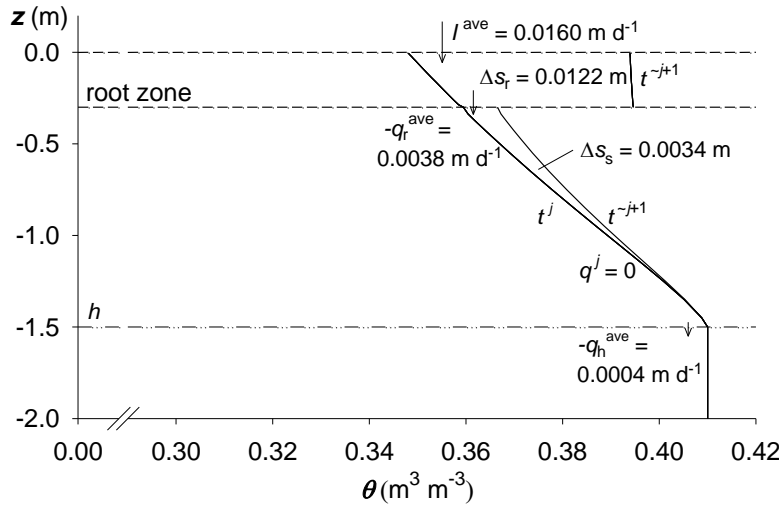


Figure 14 Numerical example for a time step of 1 d, starting from an equilibrium profile at t^j ($q^j = 0$). Indicated are the water balance terms for the ‘intermediate update’ to the moisture profile at $t^{\sim j+1}$, using the groundwater elevation of t^j . Explanation of symbols: I^{ave} is the time-averaged infiltration rate (m d^{-1}), Δs_r is the total volume change of the root zone (m), $[-q_r^{\text{ave}}]$ is the time-averaged percolation rate from the root zone (m d^{-1}), Δs_s is the total volume change of the subsoil (m), and $[-q_h^{\text{ave}}]$ is the time-averaged groundwater recharge rate (m d^{-1}).

3.3.2.3 Post-processing

In the off-line post-processing (after completing the online simulations for the whole simulation period), detailed pressure head and moisture content profiles are constructed using the functions $\mathbf{TB}\Psi_i(\psi, h)$ and $\mathbf{TB}\Theta_i(\psi, h)$ that are available for the compartments i of the schematization used by the Richards-type model. The fluxes between the compartments are found from repeated application of the water balance equation (cf. Eq. 27):

$$q_i^{\text{ave}} = q_{i+1}^{\text{ave}} - \{[\theta_i^{j+1} - \theta_i^j] / \Delta t_g + \tau_i^{\text{ave}}\} \Delta z_i \quad (31)$$

where

- q_i^{ave} = time-averaged flux density through top of compartment i (with the first one just below the soil surface) during the increment from time t^j to t^{j+1} (m d^{-1})
- Δz_i = compartment thickness (m)
- τ_i^{ave} = time-averaged root extraction rate ($\text{m}^3 \text{ m}^{-3} \text{ d}^{-1}$)

The balances can be made by starting from the top boundary condition and then proceeding downwards, or by starting from the bottom boundary condition and then proceeding upwards. If the start is made at the bottom compartment N , the value of G^{ave} (total of the time-averaged saturated flow to the column) is used for q_{N+1}^{ave} . From there on, Eq. 31 can be applied for $i = N-1, \dots, 1$.

3.4 Coupling to regional groundwater flow

3.4.1 Theory

If the modelling approach was both ‘unified’ and ‘truly three-dimensional’ then the groundwater elevation would not have to play an explicit role in the formulation in terms of equations. In our approach, there are different types of schematization for respectively the unsaturated and saturated zone:

- a one dimensional flow schematization in parallel vertical SVAT-columns in the unsaturated zone;
- a three-dimensional flow schematization in the saturated subsoil.

There are two options for the link between MetaSWAP and MODFLOW:

- *i*-link, which is a resistance-free link, meaning that the groundwater level of the SVAT unit and the head in MODFLOW cell are kept equal;
- *c*-link, which is a resistance link, involving a head difference.

The *i*-link is the most used type; the model only uses a *c*-link if the following two conditions are met:

- groundwater head above soil surface;
- availability of information about the vertical resistance of the soil surface.

An example of a *c*-link is given in the fourth column of the cross-section given in Figure 15. The link up with the regional model in this example is with the second layer of the regional model, but could also have been with the first layer.

In the case of an *i*-link the so-called groundwater recharge is a concept that can not be used without prior definition. From the viewpoint of groundwater as a *system volume* the recharge includes any water that passes ‘through’ the (moving) phreatic surface. This flux can be seen to have two components:

- the unsaturated flow driven by gradients in the unsaturated zone to/from the phreatic surface;
- the flux due to the movement of the phreatic surface itself.

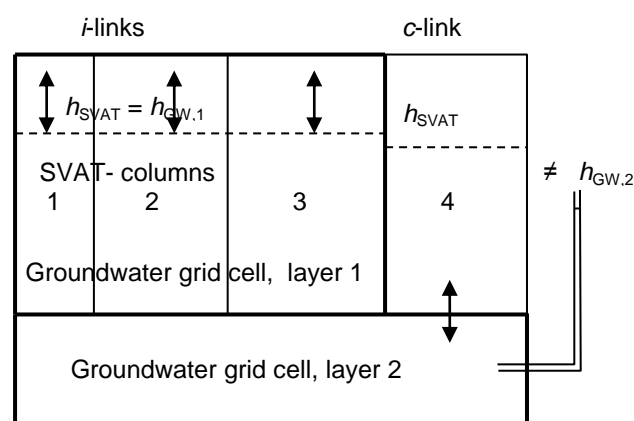


Figure 15 Cross section with examples of so-called *i*-links (column 1-3) and a *c*-link (column 4) between the SVAT-model and the regional groundwater flow model. In the case of an *i*-link the local groundwater elevation h_{SVAT} of the SVAT is equal to the groundwater head $h_{GW,1}$ in the first layer of the regional model. In the case of a *c*-link there is a head difference due to the vertical flow resistance in the saturated part of the SVAT column. In this example the *c*-link is with the second layer of the groundwater model, with head $h_{GW,2}$.

The latter requires some more explanation. Consider for instance the (theoretical) case with percolation in the unsaturated zone and with a downward saturated flux that is even stronger. Then the groundwater level will be dropping. As it drops, water of the groundwater system volume will be ‘converted’ into water belonging to the system volume of the unsaturated zone. Thus the ‘recharge’ of the groundwater will be *negative*, even though there is percolation coming from above. This is a theoretical case (because percolation will be normally be greater than the saturated flux, it is the driver), but the example does illustrate that if the coupling scheme is based on a system volume concept the recharge depends strongly on the behaviour of the phreatic surface *itself*. For this reason we prefer to not use the system volume concept as the basis for the numerical scheme. Instead, we base our scheme on a water balance method for the control volume comprising the unsaturated zone and the top part of the saturated zone, for the general case of the balance given in Eq. 26. In the implementation we avoid using the term ‘groundwater recharge’. That term we reserve for the meaning as given above. In a postprocessing step the system volume concept is used for making this recharge explicit.

3.4.2 Implementation

3.4.2.1 Water balance of coupled system

The coupling to a regional groundwater flow model involves the implementation of Eq. 26, but from a different starting point: the hypothetical case started from t^j ; here the start is from the intermediate update of the compartment pressure heads at ‘time’ t^{j+1} . Part of the recharge has already been used for the intermediate updates of these pressure heads; so this should be discounted first. This, followed by substitution of the θ -integrations given in Eq. 21 yields the so-called residual column recharge:

$$R^{\text{ave}} = R^{\text{ave}} - \frac{1}{\Delta t_g} \int_{z_s}^0 [\theta^{\sim j+1}(z) - \theta^j(z)] dz = R^{\text{ave}} - [s_r^{\sim j+1} - s_r^j + s_s^{\sim j+1} - s_s^j] / \Delta t_g \quad (32)$$

where:

- R^{ave} = column recharge of soil /ground water, time averaged (m d^{-1})
- R^{ave} = residual column recharge of soil/ground water, time averaged (m d^{-1})
- $\theta^{\sim j+1}(z)$ = volumetric water content at elevation z , after intermediate update of pressure heads at ‘time’ t^{j+1} ($\text{m}^3 \text{m}^{-3}$)
- $s_r^{\sim j+1}$ = water content of root zone after intermediate update (m)
- $s_s^{\sim j+1}$ = water content of subsoil after intermediate update (m)
- Δt_g = time increment $[t^{j+1} - t^j]$ of soil water /ground water models (d)

The water balance condition for the coupled system can then be written as:

$$\int_{z_s}^0 [\theta^{j+1}(z) - \theta^{\sim j+1}(z)] dz = [R^{\text{ave}} + G^{\text{ave}}] \Delta t_g \quad (33)$$

where:

- $\theta^{j+1}(z)$ = volumetric water content at elevation z , after update of pressure heads and phreatic level at time t^{j+1} ($\text{m}^3 \text{m}^{-3}$)
- G^{ave} = net saturated regional groundwater flow, time averaged (m d^{-1})

The integration of $\theta^{\sim j+1}(z)$ is given by $s^{\sim j+1}$, which is the sum of $s_r^{\sim j+1}$ and $s_s^{\sim j+1}$ for the storage in the root zone and the subsoil after the intermediate update of pressure heads. The integration of the (unknown) $\theta^{j+1}(z)$ is replaced by a tabular storage function $\text{TB}_{s_g}(b)$ that is derived by summing the tabular functions $\text{TB}_{s_r}(\psi, b)$ and $\text{TB}_{s_s}(\psi, b)$; the (known) intermediate update of the pressure head, $\psi_r^{\sim j+1}$, is inserted. The balance equation can now be written as:

$$\text{TB}_{s_g}(b) - s^{\sim j+1} = [R^{\text{ave}} + G^{\text{ave}}] \Delta t_g \quad (34)$$

where:

- $\text{TB}_{s_g}(b)$ = table-function for water content of the SVAT column as a function of phreatic level (m)
- $s^{\sim j+1}$ = water content of the SVAT column after intermediate update (m)

Coupling via *c*-link

The regional flow term G^{ave} can contain diverse stresses acting on the column. In the case of a so-called *c*-link (§3.4.1) the interaction with the regional groundwater model has been schematized to a purely vertical flow; the above equation can then be expanded as:

$$\mathbf{TB}_{s_g}(h) - s_k^{j+1} = [R^{\text{ave}} + q_{\text{drain}} + q_{\text{sprinkgw}} + q_{\text{bot}}] \Delta t_g \quad (35)$$

where:

R^{ave}	=	residual column recharge of soil / ground water, time averaged (m d^{-1})
q_{drain}	=	drainage (+ = to the SVAT column) (m d^{-1})
q_{sprinkgw}	=	extraction for sprinkling from phreatic layer (≤ 0) (m d^{-1})
q_{bot}	=	vertical groundwater flow (+ = to the SVAT column) (m d^{-1})

The vertical flow simulation is influenced by the phreatic level in two manners, via influences on:

- the energy head difference;
- the total flow resistance between the phreatic level and the bottom boundary of the SVAT-model.

These two influences are contained in the flow equation:

$$q_{\text{bot}} = - \frac{[h_{\text{SVAT}} - h_{\text{GW}}]}{\int_{z_i}^{h_{\text{SVAT}}} \frac{dz}{k_{\text{sat}}(z)}} \quad (36)$$

where

q_{bot}	=	vertical groundwater flow (+ = to the SVAT column) (m d^{-1})
h_{SVAT}	=	groundwater level in SVAT column (m)
h_{GW}	=	groundwater head in connected cell of groundwater model (m)
$k_{\text{sat}}(z)$	=	saturated conductivity as a function of elevation z (m d^{-1})

Coupling via *i*-link

As explained in §3.4.1 there can be several SVAT-columns coupled via zero-resistance *i*-links to a single grid cell of the groundwater model. The water balance equation in the expanded form for such a multiple-column coupling is given by:

$$\sum_{k \in K(i)} [\mathbf{TB}_{s_{g,k}}(h_{\text{GW},i}^{j+1}) - s_k^{j+1}] a_k = \{ \sum_{k \in K(i)} [R_k^{\text{ave}} + q_{\text{drain},k} + q_{\text{sprinkgw},k}] a_k + q_{\text{sat,reg},i} A_i \} \Delta t_g \quad (37)$$

where:

$\mathbf{TB}_{s_{g,k}}(h_{\text{GW},i})$	=	table-function for water content of SVAT column k as a function of groundwater elevation $h_{\text{GW},i}^{j+1}$ in groundwater grid cell i (m)
s_k^{j+1}	=	water content of SVAT column k after intermediate update (m)
a_k	=	area of SVAT unit k (m^2)
A_i	=	area of groundwater grid cell i (m^2)
$K(i)$	=	set of SVAT's k coupled to a groundwater grid cell i
R_k^{ave}	=	residual column recharge of soil/ground water of SVAT k (m d^{-1})
$q_{\text{drain},k}$	=	drainage of SVAT k (+ = to the column) (m d^{-1})
q_{sprinkgw}	=	extraction for sprinkling from phreatic layer (≤ 0) (m d^{-1})
$q_{\text{sat,reg},i}$	=	regional groundwater flow (+ = to the cell i) (m d^{-1})

3.4.2.2 Iteration scheme

Coupling via c-link

The exchange flow q_{bot} of a *c*-link is updated at the beginning of each outer loop cycle, (Figure 5). So no adjustment is made during the inner-loop iterations of the groundwater model. In order to stabilize the simulation an under-relaxation factor is used.

Coupling via i-link

With the water balance given by Eq. 37 the groundwater model has all the information that is needed for solving the coupled flow formulation, to solve for the unknown head h_i and the related saturated flow $q_{\text{sat,reg},i}$. But most groundwater models can not handle a nonlinear storage relationship. Therefore, an iteration cycle was created in which the storage characteristics are passed to the groundwater model in the form of a phreatic storage coefficient. Then Eq. 37 transforms into:

$$\sum_{k \in K(i)} \mu_k^{j+1} [h_{\text{GW},i}^{j+1} - h_{\text{GW},i}^j] a_k = \left\{ \sum_{k \in K(i)} [R_k^{\text{ave}} + q_{\text{drain},k} + q_{\text{sprinkgw},k}] a_k + q_{\text{sat,reg},i} A_i \right\} \Delta t_g \quad (38)$$

where μ_k^{j+1} is the dynamically determined phreatic storage coefficient ($\text{m}^3 \text{m}^{-2} \text{m}^{-1}$). For the converged situation, the coefficient is given by the slope of the chord between two points on the storage curve:

$$\mu_k^{j+1} = [s_k^{j+1} - s_k^{j+1}] / [h_{\text{SVAT},k}^{j+1} - h_{\text{SVAT},k}^j] \quad (39)$$

For the numerical example given in §3.3.2.2, the obtained storage table-function $\text{TB}_{s_g}(h)$ is given in Figure 16. The function has been extended above the soil surface, assuming a storage coefficient of 1.0 for ‘ponded groundwater’. In the non-converged situation of the p th-iteration, the newest groundwater head iteration $h_{\text{GW},i}^{j+1,p}$ and the newest total storage $s_k^{j+1,p}$ (total of the storage in the control volumes of root zone and subsoil) do not form a point on the storage curve. Figure 16 shows two options for updating the phreatic storage coefficient during the iteration process. The first option is to use Eq. 39 even though there is a discrepancy between the latest groundwater head $h_{\text{GW},i}^{j+1,p}$ and the latest $h_{\text{SVAT},k}^{j+1,p}$. The latter is obtained via the water balance (including the saturated flow G) and an inverse look-up operation in the storage table $\text{TB}_{s_g}(h)$, by using its inverse form $\text{TB}h_{g,k}(s)$. Since it is based on the water balance we call it the *storage-based* storage coefficient:

$$\mu_{s,k}^{j+1,p+1} = [s_k^{j+1,p} - s_k^{j+1}] / [\text{TB}h_{g,k}(s_k^{j+1,p}) - h_{\text{SVAT},k}^j] \quad (40)$$

where

$\mu_{s,k}^{j+1,p+1}$ = storage-based storage coefficient for the next cycle $p+1$ ($\text{m}^3 \text{m}^{-2} \text{d}^{-1}$)

$\text{TB}h_{g,k}(s)$ = table-function of phreatic level as a function of storage (m)

The so-called *level-based* storage coefficient $\mu_{h,k}^{j+1,p+1}$ uses the latest *groundwater head* in combination with its corresponding storage value for finding the slope of the chord:

$$\mu_{h,k}^{j+1,p+1} = [\text{TB}h_{g,k}(h_{\text{GW},i}^{j+1,p}) - s_k^{j+1}] / [h_{\text{GW},i}^{j+1,p} - h_{\text{SVAT},k}^j] \quad (41)$$

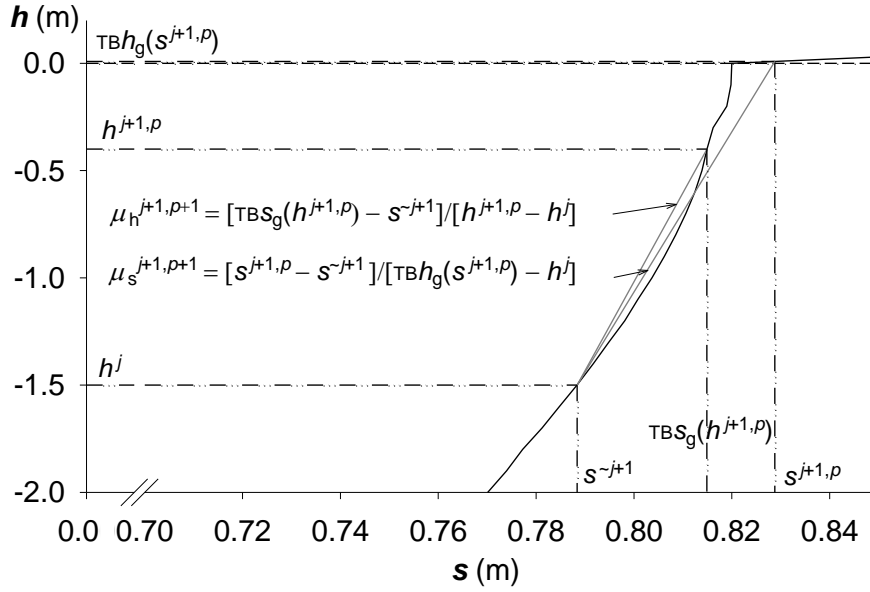


Figure 16 Example of a storage function $TB_{sg}(h)$ and its inverse $TB_{hg}(s)$, showing two options for updating the storage coefficient of the groundwater model. Explanation of symbols: h^j is the groundwater elevation at time t^j , $h^{j+1,p}$ is the p -th iteration for the groundwater elevation at t^{j+1} , s^{-j+1} is the 'intermediate update' of the total water storage at t^{j+1} , $s^{j+1,p}$ is the p -th iteration for the storage at t^{j+1} , $\mu_h^{j+1,p+1}$ is the $(p+1)$ th iteration for the level-based storage coefficient, $\mu_s^{j+1,p+1}$ is the $(p+1)$ th iteration for the storage-based storage coefficient

The level-based storage coefficient is the standard option in the numerical scheme. The second option is mainly employed for handling the nonlinear transition of the storage relationship at the soil surface, to avoid oscillations of h between iterations.

Apart from the transition to the ponding situation on the soil surface, a sudden drop of the groundwater level can also give rise to instability of the scheme. The stabilization strategy is in this case to assume a certain amount of 'drag down' of the pressure heads due to the falling groundwater level. If for instance the level starts at the soil surface, then we assume that there is 1:1 drag down of the pressure heads due to the falling groundwater level. This then results in an equilibrium profile. In for instance a situation with percolation and falling groundwater level, we first compute what the percolation would become if the final value of pressure head remains the same as after the 'intermediate' update. To avoid that the falling groundwater level induces a large percolation pulse during the next time step, we adjust the current pressure head in such a manner that the anticipated increase of the percolation during the next time step is partly made to occur during the *current* step. Such stabilization strategies are encoded in the table-function of the column storage before the cycle involving the groundwater model is started.

In the multiple-column coupling to a single groundwater cell, Eq. 38 contains a summation of [storage coefficients]*[areas] of the individual columns. In the used OpenMI style coupling scheme these summations are realized via the mapping table between SVAT units and groundwater grid cells. By passing the storage coefficients to the groundwater model in the dimension $[L^3 L^{-1}]$ the groundwater model does not have to know the separate areas of the SVATs; in this dimension the coefficients can simply be added up, yielding the storage coefficient for the groundwater grid cell.

The cycle for the coupling scheme is summarized in the lower half of Figure 5. Full convergence of an iteration scheme is often not desired, because the achieved extra numerical accuracy is not worth the required computational effort. But of course it is crucial to have a correction mechanism that gets the models ‘back on track’ as soon as possible during the ensuing time step(s), thus bringing the groundwater head and the phreatic level of in the SVAT together again. This is done in the following manner. A deviation is compensated during the next time step by purposefully making a similar head error, but then with the *opposite* sign. This is illustrated with a case where the groundwater head of the preceding cycle ended at level below that of the SVAT model. The storage coefficient is computed for the chord from the initial (‘old’) point involving the head of the groundwater model of the previous time step to the ‘new’ point involving the phreatic for the iteration cycle of the new time step. In Figure 17 this calculation is illustrated for the balance-based storage coefficient. The water balance deviation of the starting point is compensated for by adding a correction term to the residual recharge that is passed to the groundwater model:

$$R_k^{\text{ave}} = R_k^{\text{ave}} + [s_k^{\sim j+1} - \text{TB}_{s_{g,k}}(h_{\text{GW},i}^j)] \quad (42)$$

where:

- R_k^{ave} = residual column recharge of soil / ground water from SVAT k (m d^{-1})
- R_k^{ave} = adjusted residual column recharge of soil / ground water from SVAT k (m d^{-1})
- $s_k^{\sim j+1}$ = water content of SVAT k after intermediate update (m)
- $h_{\text{GW},i}^j$ = groundwater head in cell i connected to SVAT k (m)
- $\text{TB}_{s_{g,k}}(h)$ = table-function giving water content of SVAT column k as a function of the groundwater elevation h (m)

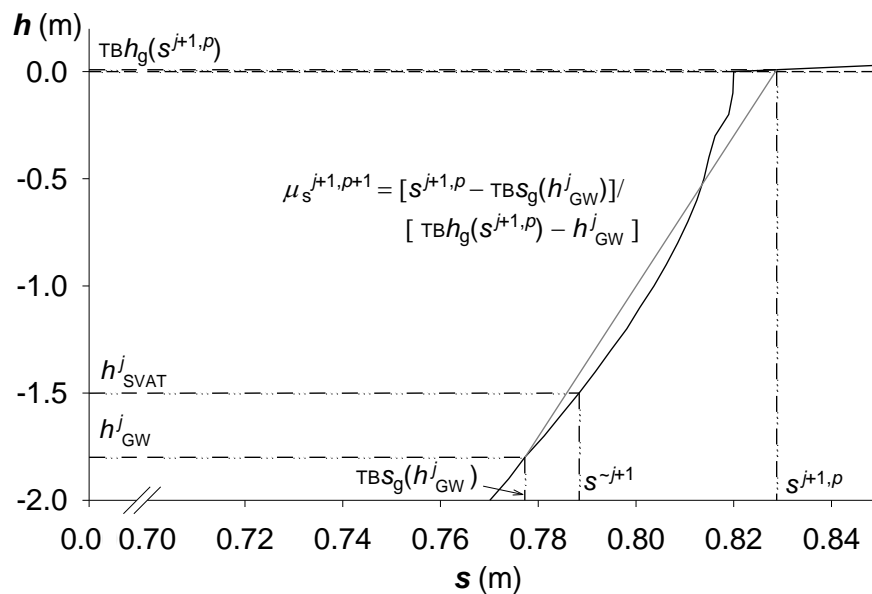


Figure 17 Storage coefficient calculation for a case with a deviation between the initial phreatic level in the SVAT model (h_{SVAT}^j) and the initial groundwater head (h_{GW}^j). The example is for the balance-based storage coefficient. The difference with the storage-based storage coefficient is similar to what is shown in Figure 16.

So the correction is done ‘on the fly’ in the course of the calculations for the new time step: not the groundwater head itself is corrected, but the *change* of the groundwater head during the next time step. The algorithm supplies the groundwater model with a consistent combination of adjusted storage characteristics and recharge: the correction component of the recharge exactly fits the storage difference between the (deviating) initial groundwater head and the initial groundwater elevation of the SVAT. The effect on the water balance is *indirect*: by bringing the head of the groundwater model back into line with the level in the SVAT the saturated *flow* will be affected, and thus also the groundwater elevation in the SVAT and subsequently the head the groundwater model.

3.4.2.3 Post-processing

For interpreting the model simulation and for groundwater quality studies it can be of interest to obtain the recharge as seen from the viewpoint of groundwater as a system volume, as explained in §3.4.1. The water balance terms are then defined as in Figure 18. In this case we assume that the storage coefficient follows directly from the *saturated* water content profile of the groundwater column. It is calculated with:

$$\mu_{\text{sat}} = \frac{1}{b^{j+1} - b^j} \int_{b^j}^{b^{j+1}} \theta_{\text{sat}}(z) dz \quad (43)$$

where:

- μ_{sat} = storage coefficient of groundwater body as a system volume ($\text{m}^3 \text{m}^{-2} \text{d}^{-1}$)
- b^j = groundwater head at time level j (m)
- $\theta_{\text{sat}}(z)$ = saturated volumetric water content at elevation z ($\text{m}^3 \text{m}^{-3}$)

The water balance of the groundwater as a system volume is given by

$$\Delta S = \mu_{\text{sat}} [b^{j+1} - b^j] = (R + G) \Delta t \quad (44)$$

where:

- ΔS = storage change of groundwater body (m)
- R = recharge based on the system volume concept (m d^{-1})
- G = groundwater flow (m d^{-1})

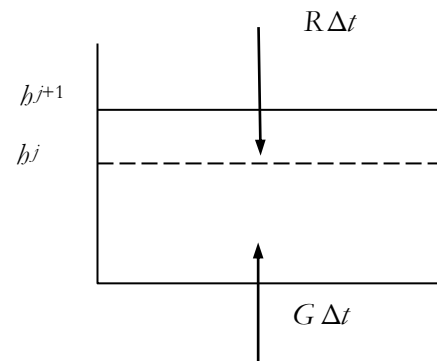


Figure 18 Definition of fluxes near the groundwater level for making a water balance of groundwater as a system volume. Explanation of symbols: b^j is the groundwater head at time level j , R is the groundwater recharge based on the system volume concept, G is the net groundwater flux and Δt is the time step

The water balance of the groundwater as a system volume is given by

$$\Delta S = \mu_{\text{sat}}[b^{j+1} - b^j] = (R + G)\Delta t \quad (45)$$

where:

- ΔS = storage change of groundwater body (m)
- R = recharge based on the system volume concept (m d⁻¹)
- G = groundwater flow (m d⁻¹)

The groundwater level change is known from the simulation based on the control volume concept. The recharge based on the system volume concept can be made explicit by rearranging the above equation:

$$R = \mu_{\text{sat}}[b^{j+1} - b^j] / \Delta t - G \quad (46)$$

3.5 Data summary

For describing the processes on the soil surface, parameters are needed for

- maximum infiltration rate;
- the microstorage capacity.

For the unsaturated flow the soil physical metafunctions should be supplied for:

- the percolation/capillary rise;
- the storage in the root zone (box 1);
- the storage in the subsoil (box 2)

These functions should be given in tabular form, for discrete steps of:

- the root zone depth;
- the soil water content;
- the phreatic level.

The given function values are then used as vertices of piece-wise linear functions.

The functions can include the influence of macroporosity on the storage characteristics. In the postprocessing of solutions provided by 'SWAPsteady' (Appendix A) the macroporosity is superimposed on the storage in the steady-state solutions. This is done with the simple computational rule that the filling of the macroporosity with water depends only on the groundwater level.

4 Drainage

4.1 Introduction

The SIMGRO code does not anymore include the regional groundwater flow. But since it does include the local flows to drainage media a short excursion into the theory of groundwater flow is justified as an introduction to the presented drainage formulae.

4.2 Theory

Darcy's Law for the flow of a homogeneous incompressible fluid through a porous medium can be generalized to the three-dimensional form given by (e.g. Bear 1979):

$$\mathbf{q} = \mathbf{K} \cdot \mathbf{J} = -\mathbf{K} \cdot \text{grad } h \quad (47)$$

where:

- \mathbf{q} = the specific discharge vector (m d^{-1})
- \mathbf{K} = the so-called conductivity tensor (m d^{-1})
- h = hydraulic head (m)
- \mathbf{J} = $-\text{grad } \varphi$, the hydraulic gradient with components $J_x = -\partial h / \partial x$, $J_y = -\partial h / \partial y$, and $J_z = -\partial h / \partial z$ (-)

The conductivity tensor \mathbf{K} is symmetric (see e.g. Bear , 1979). And in the case that x, y , and z -axes are (through a transformation) made to correspond with the principal directions of the anisotropic medium, only the elements on the diagonal are non-zero, i.e. K_{xx}, K_{yy}, K_{zz} . In the following these symbols will be abbreviated to K_x, K_y, K_z .

The equation of motion given by Eq. 47 just describes the flow in a point. (Strictly speaking that is not true, of course, due to the irregularities of the soil matrix. But use of the 'representative elementary volume'-concept, allows us to describe the flow in terms of continuum mechanics). For making it operational at a finite scale it has to be combined with the mass conservation equation. It then becomes possible to scale up the flow description to a domain of finite dimensions that is embedded in the surrounding environment by means of boundary conditions. The SIMGRO-model is intended for describing the flow at the scale of a drainage basin. That also requires describing the local flows to watercourses and wells. But the embedding of detailed descriptions of the local flows in the regional model would not be practical. In order to arrive at a manageable formulation we decompose the flow into:

- regional flow components that are described explicitly;
- local flow components that are described using metafunctions.

We derive the local-flow metafunctions by solving subproblems for the local flows. These subproblems are stated in such a manner that they take place within local subdomains, involving zero-flux boundaries in the horizontal direction. It is then possible to superimpose the local flow formulations on the regional flow, by simply adding the metafunctions as extra leakage terms to the regional flow equation.

Drainage to a watercourse is a gravity flow involving relatively small differences in the hydraulic head. The head differences depend very much on the preceding history of events, involving the precipitation, and so on. So the involved fluxes must be simulated through time.

In the sense that was expounded in §4.2 the flows to watercourses can be seen as 'local' if there is a surface water system involving parallel watercourses at equal spacing, in the presence of a uniformly distributed recharge from the unsaturated zone to the groundwater: in that case the drainage can be seen as a diffuse process that is 'spread over' the local-flow subdomain, with no boundary effects to the regional system. But the conceptualization of the regional model should of course be capable of dealing with situations that differ from the mentioned one. Before going into that, the schematized situation will be discussed first.

In order to arrive at a manageable numerical implementation for the computation of drainage fluxes a number of simplifying assumptions are made. The first is that the local flow can be adequately described as a stream of steady-state situations, like is done for the soil water modelling. This assumption neglects the fast-flow terms that are present if the shallow groundwater receives a heavy percolation pulse. The fast flow terms are due to the locally steep hydraulic gradient in the direct vicinity of the watercourse, involving a more 'square' shape of the water table than under steady-state conditions. These terms were given by for instance Dumm (1954), and Kraijenhoff van de Leur (1958).

The second main assumption is that the local flow can be decomposed, using the method given by Ernst (1962), as adapted by Van der Molen (1972). The decomposition involves the following components, which are illustrated in Figure 19 (adapted from Jousma and Massop, 1996):

- vertical flow from where the percolation water enters the groundwater body, to the 'main stream' of the aquifer;
- essentially horizontal flow in the aquifer towards the watercourse;
- radial flow in the vicinity of the watercourse;
- entrance flow to the watercourse itself (Van der Molen, 1972).

The assumption is that the total hydraulic head difference between the local groundwater culmination point and the water level in the watercourse can be written as the sum of the head differences for the separate flow components:

$$\Delta h = \Delta h_v + \Delta h_h + \Delta h_r + \Delta h_e \quad (48)$$

where:

- Δh = total head difference between groundwater culmination point and surface water level (m)
- Δh_v = head difference for vertical flow to the 'main stream' of the aquifer (m)
- Δh_h = head difference for horizontal flow to watercourse (m)
- Δh_r = head difference for radial flow to watercourse (m)
- Δh_e = head difference for entrance flow to watercourse (m)

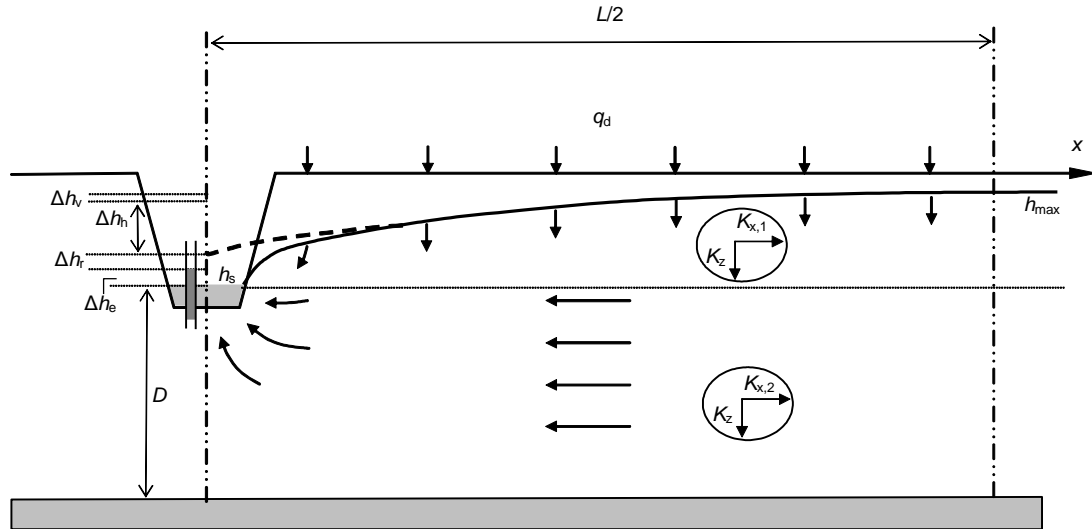


Figure 19 Decomposition of the head loss in the flow towards a watercourse, according to Ernst (1962) and Van der Molen (1972); figure adapted from Jousma and Massop (1996).

The conceptualization thus involves four flow resistances that are connected ‘in series’. That is of course an approximation. There is for instance an overlap between the horizontal flow and the radial flow, involving the same part of the flow domain. Here we give the flow formulation for parallel watercourses. The geometry of the flow situation is governed by the following parameters:

- L = distance between the parallel watercourses (m)
- D = thickness of the aquifer below the drainage base (m)
- P = wetted perimeter of a watercourse (m)

For the horizontal conductivity a distinction is made between the subdomain above the drainage base ($K_{x,1}$) and the subdomain below it ($K_{x,2}$).

In order to ‘feed’ the lateral flow in the aquifer, the vertical flow must on average travel a distance of $D/2$ (disregarding the flow above the drainage base). Using the one-dimensional form of Eq. 47, and integrating over the interval $[0; D/2]$, the head difference for the vertical flow can then simply be computed with:

$$\Delta h_v = \frac{q_d D/2}{K_z} = q_d L \omega_v; \quad \omega_v = \frac{D/2}{L K_z} \quad (49)$$

where:

- q_d = drainage flux (sign positive for flow towards the watercourse) (m d^{-1})
- K_z = vertical conductivity (m d^{-1})
- ω_v = vertical drainage resistance (d m^{-1})

In situations where the drainage flux stems from upward seepage through the semi-pervious layer that in Figure 19 forms the lower ‘boundary’ of the flow domain, the vertical flow resistance is already taken into account in the regional flow equation. In such a situation the head loss given by Eq. 49 should be left out, to avoid double counting of this flow resistance.

For the horizontal flow between parallel watercourses the flow equation reduces to a one-dimensional form, with only the steady-state drainage term. This equation is also known as the Dupuit discharge formula (e.g. Bear, 1979). Here it is written as:

$$-\text{div } \mathbf{q}^a = \frac{d}{dx} \left([b(x) - D] K_{x,1} \frac{db}{dx} + D K_{x,2} \frac{db}{dx} \right) = q_d \quad (50)$$

where:

- \mathbf{q}^a = specific discharge vector (m d⁻¹)
- q_d = drainage flux (sign positive for flow towards the watercourse) (m d⁻¹)
- $b(x)$ = hydraulic head at horizontal distance x from the ditch, with reference to the bottom of the aquifer (m)

The sign of the drainage term q_d is positive for flow to surface water. If the breadth of the watercourse itself is neglected, integration between $x=0$ and $x=L/2$, and insertion of the boundary condition $b(0)=b_s$, then yields

$$b(x) = b_s + \sqrt{D^2 \frac{K_{x,2}^2}{K_{x,1}^2} + \frac{q_d}{K_{x,1}} (xL - x^2)} - D \frac{K_{x,2}}{K_{x,1}} \quad (51)$$

Inserting $x=L/2$ yields the head elevation at the culmination point (b_{\max}), and thus the head difference for the horizontal flow:

$$\Delta b_h = b_{\max} - b_s = b(L/2) - b_s = \sqrt{D^2 \frac{K_{x,2}^2}{K_{x,1}^2} + \frac{q_d L^2}{4K_{x,1}}} - D \frac{K_{x,2}}{K_{x,1}} \quad (52)$$

with the horizontal drainage resistance ω_h (d m⁻¹) given by:

$$\omega_h = \frac{\Delta b_h}{q_d L} = \frac{1}{q_d L} \left(\sqrt{D^2 \frac{K_{x,2}^2}{K_{x,1}^2} + \frac{q_d L^2}{4K_{x,1}}} - D \frac{K_{x,2}}{K_{x,1}} \right) \quad (53)$$

The expression for the drainage flux as a function of the head difference can be made explicit by rearranging Eq. 52:

$$q_d = \frac{8K_{x,2}D}{L^2} \Delta b_h + \frac{4K_{x,1}}{L^2} \Delta b_h^2 \quad (54)$$

For implementation in the model the mean head-elevation is also needed; it is given by:

$$\bar{b} - b_s = \frac{\sqrt{\frac{K_{x,1}}{q_d} \frac{K_{x,2}^2}{K_{x,1}^2} D^2} + \sqrt{\frac{q_d}{K_{x,1}} \frac{L^2}{4}}}{L} \arctan \left(\sqrt{\frac{q_d}{K_{x,1}}} \frac{K_{x,1} L}{2K_{x,2} D} \right) - \frac{K_{x,2} D}{2K_{x,1}} \quad (55)$$

The ratio between the mean head difference and Δh_h is commonly referred to as the *form factor* (Ernst, 1983):

$$\zeta_h = \frac{h - h_s}{h_{\max} - h_s} \quad (56)$$

which in the simplified case of only flow below the drainage base (i.e. neglecting the quadratic term in Eq. 54) is equal to 2/3. For situations where also the radial and entrance flow resistance play a role, the form factor assumes higher values. In the extreme case of no vertical or horizontal resistance ($\Delta h_v = \Delta h_h = 0$) the form factor equals unity.

For the radial flow to a watercourse Ernst (1962) gives:

$$\Delta h_r = \frac{q_d L}{\pi K_e} \ln \left(\frac{\alpha D_e}{P_e} \right) = q_d L \omega_r; \quad \omega_r = \frac{1}{\pi K_e} \ln \left(\frac{\alpha D_e}{P_e} \right) \quad (57)$$

where ω_r is called the radial drainage resistance ($d \cdot m^{-1}$), and α is a geometry factor that depends on the specific configuration of the aquifer in relation to the watercourse. In the presence of anisotropy, the value of the conductivity in the equivalent isotropic domain is taken as $\sqrt{(K_x K_z)}$. The D -value has then to be transformed with: $D_e = D \sqrt{(K_x / K_z)}$; assuming that the wetted perimeter is mostly in the x -direction, the P -value has to be transformed with $P_e = P \sqrt{(K_z / K_x)}$. The relevant expressions for field drains are e.g. given by Van der Molen (1972).

For the entrance flow Van der Molen (1972) gives:

$$\Delta h_e = q_d \left(\frac{c_b L}{P} \right) = q_d L \omega_e; \quad \omega_e = \frac{c_b}{P} \quad (58)$$

where c_b is the local entrance resistance (d), and ω_e the entrance resistance ($d \cdot m^{-1}$). This description of radial and entrance resistance neglects the presence of a seepage face in the watercourse, just above the surface water level.

Summarizing, the total head difference for the mean head between the watercourses can be written as:

$$\bar{h} - h_s = q_d L (\omega_v + \zeta_h \omega_h + \omega_r + \omega_e) \quad (59)$$

and for the culmination point between the watercourses the head difference can be written as:

$$h_{\max} - h_s = q_d L (\omega_v + \omega_h + \omega_r + \omega_e) \quad (60)$$

For deep watercourses, it is assumed that the above given drainage theory can also be applied to the deeper layers of the geohydrologic schematization that are cut into by the watercourses. This should not be considered equivalent to applying a multi-layer drainage formula, like given in Appendix 1. For situations with relatively small vertical resistances to the subsoil, it is relevant to use a multi-layer drainage formula for the *local* flow: the

drainage water seeks a route with the lowest flow resistance, which can mean ‘taking a detour over the highway’ in the deeper subsoil. Since this flow takes place *within* the local subdomain, it is not a flow that is modelled by the regional flow equation: the local flow is superimposed upon the regional one. In comparison to a single layer formula, that can lead to a substantial decrease of the computed drainage resistance.

The above given derivations are for a uniformly distributed recharge situation, which also applies to situations with seepage from a leaky layer. In a regional model all kinds of different situations can occur, of course. The question is whether the above given approach can then still be used. Consider for instance the situation with zero recharge and regional flow that is locally drained. Depending on the strength of the regional flux, the horizontal drainage resistance of the local flow can vary. It thus should be realized that the used approach is an approximate one.

When the groundwater level starts to approach the mean soil surface, the lowest-lying places start to act as a drainage medium. With increasing level, more parts become inundated, thus leading to a sharp reduction of the horizontal flow resistance. Also the radial resistance and entrance resistance show a sharp decrease, due to the increase of the wetted perimeter involved in the inundation.

4.3 Model implementation

As regards the drainage flow to watercourses, the flow description given in §4.2 was for the theoretical situation with parallel watercourses that have an equal spacing L . In practice, the model spatial units are criss-crossed by watercourses having varying dimensions, like in the example of Figure 20. A certain watercourse is active as a drainage or infiltration medium if either the groundwater level or the surface water level is higher than the elevation of the bottom of the watercourse, and if the levels differ from each other. In order to apply the given theory in §4.2, several adaptations are required.

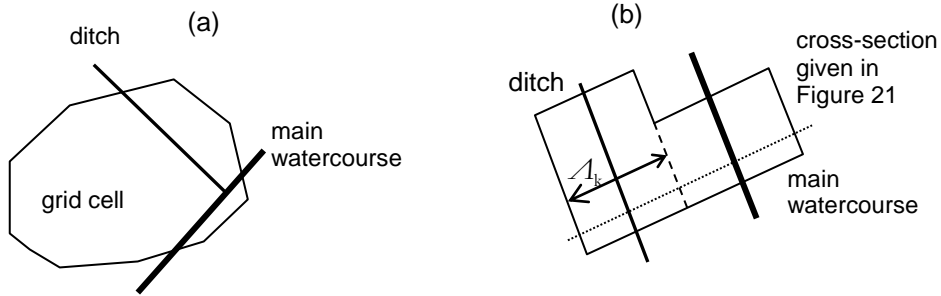


Figure 20 Example of a model spatial unit that is criss-crossed by watercourses having vary dimensions: practical situation (a), and schematised situation used in the calculation method (b)

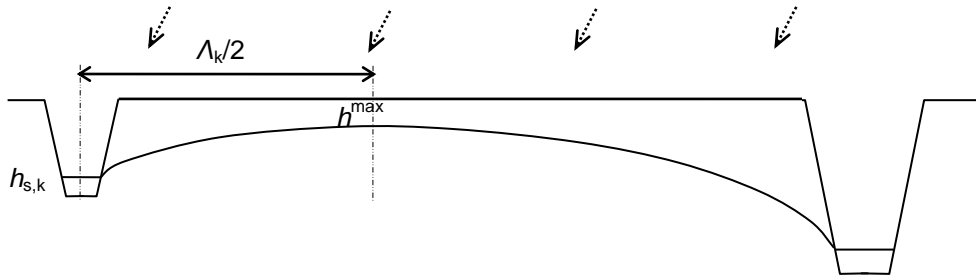


Figure 21 Example of a cross-section of the shallow groundwater for a situation with simultaneous drainage flow to a ditch and a main watercourse (see also Figure 20)

The first adaptation is to group the watercourses into a number of categories k , having similar characteristics in terms of:

- the cross-section;
- the entrance resistance;
- surface water level.

Obviously, in practical situations the watercourses are not parallel, and different types can be present. For such situations it is only possible to compute an ‘equivalent’ spacing, by dividing the area of a subdomain through the length of watercourse (Ernst, 1978):

$$L_k = \frac{A_i}{l_k} \quad (61)$$

where:

L_k = equivalent spacing of watercourses in category k (m)

A_i = area of model spatial unit (m^2)

l_k = total length of watercourses in category k (m)

Ernst (1978) presents and discusses a method for using the equivalent drainage spacing in a regional analysis of different flows to watercourses of varying cross-sections and spacings. The method takes into account the interdependency of the drainage flows to the different categories of watercourses. The route a water droplet takes within the groundwater body depends on the total configuration. Even though the method of Ernst (1978) is theoretically sound, it is not used here. Instead, we use an alternative approach that accounts for combinations of simultaneous infiltration and drainage and for the arising combinations of head losses due to ‘horizontal’ and ‘radial’ flows.

Our approach involves the introduction of an entity the ‘drainage influence span’ as a function of the relative strength of the drainage flux towards a certain category of water courses. For this we first compute the ‘drainage subarea’ a_k of each category of watercourses according to

$$a_k = \frac{|\mathcal{Q}_{d,k}|}{\sum |\mathcal{Q}_{d,k}|} \mathcal{A}_i \quad (62)$$

where $\mathcal{Q}_{d,k}$ is the drainage flux to category of watercourses k within the spatial unit in [$\text{m}^3 \text{d}^{-1}$]. The underlying assumption of Eq. 62 is a uniformly distributed recharge over the spatial unit, whatever the circumstances and the type of drainage medium that is involved (small/large watercourse). The absolute values are used, because it is also possible that infiltration takes place instead of drainage. And, even more complex, it is possible that both drainage and infiltration take place *simultaneously* within the same spatial unit. Both directions of flow ‘need’ a certain part of the soil volume for the flow, so in that sense both are competing for use of the (same) flow medium. For situations with a relatively high density of watercourses, this method entails that the situation in a spatial unit is schematized to that of (b) in Figure 20. For each of the watercourse categories, the mean ‘drainage influence span’ can now be calculated with

$$\mathcal{A}_k = \frac{a_k}{l_k} \quad (63)$$

For situations with $\mathcal{A}_k > \sqrt{\mathcal{A}_i}$ the schematization as given in Figure 20 becomes unrealistic, due to the sideways-elongated form of the drainage subarea. That would lead to an *over*-estimate of the horizontal drainage resistance, because the water would have to travel an unrealistic distance in the local flow system. (This does not, however, apply to the radial and entrance resistance. The reason for the horizontal resistance being different is that \mathcal{A} itself is in the expression for it, as is evident from Eq. 53. But \mathcal{A} is not present in the expressions for the other resistances, as given in Eq. 57 for the radial resistance and Eq. 58 for the entrance resistance.)

Like in the computation of the vertical leakage flux densities we consider the groundwater level h as a *mean* level within the spatial unit. In the case that this level is higher than the bottom of a watercourse, one can be sure that the watercourse is active, either involving infiltration or drainage. In the case that the level is below the deepest bottom, one can be sure that *none* of the watercourses will be draining. But it is not always so clear-cut. The intermediate situation can occur with a watercourse actively draining, even though the *mean* groundwater level is below the bottom of that watercourse. That this possibility exists has to do with the local head variation caused by the

horizontal drainage resistance. For this reason the drainage calculation method also includes the calculation of the (unknown) h^{\max} , which is the maximum (local) ground-water level within a spatial unit. Put more precisely, that is the level at the culmination point between two watercourses. Examples of cross-sections of the shallow groundwater are given in Figure 21 for the line indicated in Figure 20. It is assumed that h^{\max} is the same for all of the drainage subareas, which is of course an approximation. In order to compute it, we first formulate the drainage flow equations as if we already know its value, and also the (as yet unknown) \mathcal{A}_k 's.

For a given h^{\max} and \mathcal{A}_k the drainage flux to a category of water courses k can be computed as (cf. Eq. 60):

$$Q_{d,k} = l_k \mathcal{A}_k q_{d,k} = l_k \frac{h^{\max} - h_{s,k}}{\omega_{v,k} + \omega_{h,k} + \omega_{r,k} + \omega_{e,k}} \quad (64)$$

where $h_{s,k}$ is the surface water level in water courses of category k , the drainage base. Subsequently we can compute the mean head elevation within the drainage subarea a_k of the spatial unit with (cf. Eq. 59):

$$h_k^m = h_{s,k} + \frac{Q_{d,k}}{l_k} (\omega_{v,k} + \zeta_{h,k} \omega_{h,k} + \omega_{r,k} + \omega_{e,k}) \quad (65)$$

where $\zeta_{h,k}$ is the form factor for the horizontal drainage flow of watercourses in category k . The weighted mean of h_k^m should be equal to the mean groundwater level h in the spatial unit:

$$\frac{1}{\mathcal{A}_i} \sum a_k h_k^m = h \quad (66)$$

In the calculation procedure we have to solve for the following principal unknowns: h^{\max} and the \mathcal{A}_k 's. (The Q_d 's are of course also unknowns, but follow directly from Eq. 64.) For the solution we use an iterative scheme. In the initial step of the very first calculation, we assume that all the categories of watercourses have the same 'drainage influence span', as given by:

$$\mathcal{A}_k^o = \frac{\mathcal{A}_i}{\sum_k l_k} \quad (67)$$

For the next steps of the calculation (and for new time steps), we simply use the last value as a starting point. The iterative scheme involves the following steps:

1. Perform the initialization of the $Q_{d,k}$'s and the head at the culmination point h^{\max} .
2. Compute the drainage spans A_k using Eq. 63.
3. Compute the horizontal drainage resistances ω_h and the total drainage resistance.
4. Compute the $Q_{d,k}$, the mean head h_k^m within each drainage subareas using Eq. 65
5. Compute the mean groundwater level in the spatial unit h^{mj} , using Eq. 66.
6. Compare the value of h^{mj} with the value h of the regional model. If convergence of h^{mj} has been reached, then **stop**, otherwise **continue**.
7. If h^{mj} is higher than h , then lower the estimate of h^{\max} , or conversely raise h^{\max} if h^{mj} is too low. The adjustments are made using a relaxation factor for predicting the effect of a change in h^{\max} on h^{mj} .
8. Go to step 2.

Since the drainage flux is recomputed for each surface water time step, the strict adherence to the above scheme could lead to a large increase of the computational burden. In order to avoid this, a pragmatic approach is followed, involving at most two iteration cycles per surface water time step.

4.4 Data summary

The input data of the geohydrologic schematization consist of the following parameters given per grid cell of the groundwater model:

- thickness of the layers;
- conductivities in the xy -plane for aquifers, xz -plane for aquitards.

Boundary conditions can be supplied in the form of heads or net fluxes within all nodes of the domain. The flow to a well can either involve a head or a flux boundary condition. In the latter case we assume that it is always possible to extract the desired amount. In order for this assumption to be valid, a separate analysis is required for the detailed situation around a well. The extractions are converted to 'diffuse' flux densities (dividing by area of spatial unit).

Drainage characteristics of watercourse categories are supplied in the form of a long list, along with the geometry in the separate units. The watercourses themselves are described in §5. Here it is relevant to note that a distinction is made between:

- watercourses in the conventional sense, with a cross-section; for these the drainage characteristics given in terms of:
 - entrance resistance and radial resistance;
 - horizontal resistance; this resistance is optional, because it can also be dynamically computed by the model from the basic data (geometry and subsoil conductivities) using the iterative scheme given above;
- field drains, with a radius instead of cross-section; the same resistance data as for water courses;
- gulleys, with the drainage characteristics given in terms of a total drainage resistance for the situation when the gulleys just start draining;
- soil surface, with a drainage depth of zero, and a very low drainage resistance (<1 d).

5 Surface water

5.1 Introduction

Surface water plays a key role in the functioning of many regional hydrologic systems. The interaction with the soil water and groundwater can be very complex, especially in situations with water on the soil surface.

The integrated modelling concept for water on the soil surface takes account of its ‘multiple identity’ as:

- ponding water that takes part in the top system processes (evaporation) and that can infiltrate into the soil column;
- phreatic groundwater if there is contact with the regional groundwater body.
- surface water that is in contact with the channel network.

The role as ponding water is described in §**Error! Reference source not found.** and §3.2, the role as ‘visible groundwater’ in §3.4. In these descriptions a ‘reservoir’ approach is followed, i.e. not involving any horizontal gradients. Large-scale lateral movement of surface water is assumed to take place through a network of conduits that forms part of the model schematization. In the following section, we will confine ourselves to this channel flow. In §5.3.3 the implementation of the integrated concept for water on the soil surface is described.

5.2 Theory

Using the full form of the Saint Venant equations (non-steady gradually varied flow in open conduits) for the whole channel network would lead to an unwieldy integrated model: compared to the soil water and groundwater submodels the surface water model would require a disproportionate amount of computational effort. Therefore a flexible modelling concept is used, involving a simplified model for the smaller channels and a hydraulic model for the larger ones. Here we confine ourselves to describing the simplified concept.

Just like in the soil-water modelling, the dynamics of surface water are simulated with a quasi-steady state method, using a stream of steady-state situations. For the steady states we assume gradually varied non-uniform flow. The momentum equation can for instance be stated as (Chow, 1959)

$$\frac{dy}{dx} = \frac{S_o - Q^2 / C^2 A_f^2 R}{1 - a Q^2 / g A_f^2 D_h} \quad (68)$$

and the continuity (for steady-state flow) as

$$\frac{dQ}{dx} = q_{\text{lat}} \quad (69)$$

where:

x	=	distance along the watercourse (m)
y	=	water depth (m)
z	=	elevation of the channel bottom (m)
S_o	=	slope of the channel bottom, dz/dx (-)
Q	=	discharge ($\text{m}^3 \text{s}^{-1}$)
α	=	energy coefficient (-)
g	=	acceleration due to gravity ($\text{m}^2 \text{s}^{-1}$)
C	=	Chézy coefficient ($\text{m}^{1/2} \text{s}^{-1}$)
A_f	=	cross-sectional area of the water normal to the direction of flow (m^2)
R	=	hydraulic radius (A_f divided by the wetted perimeter) (m)
D_h	=	hydraulic depth (A_f divided by the width of the free surface) (m)
q_{lat}	=	lateral inflow per unit of length of the channel ($\text{m}^2 \text{s}^{-1}$)

For handling Eq. 68 we use a dynamic metamodeling method: it is first solved in the ‘pre-processing’ stage using a hydraulic model, covering a wide range of boundary conditions. The results are then stored and subsequently used in the form of hydraulic metafunctions. The transitions between the steady-state flow situations are calculated using the continuity equation in the form of:

$$\frac{\partial A_f}{\partial t} + \frac{\partial Q}{\partial x} = q_{\text{lat}} \quad (70)$$

5.3 Model implementation

5.3.1 Schematization and hydraulic metafunctions for channel flow

The watercourses are divided into trajectories. Structures are assumed located at the end of a trajectory, with the simulated water level pertaining to the upstream situation just before the end. Depending on the detail of the implementation the explicitly modelled watercourses can involve even the smallest of ditches.

For a given schematization of watercourses the storage function is used in the form of:

$$S_n = \Xi_n(h_{s,n}) \quad (71)$$

where S (value) and Ξ (function) represent the storage in the watercourse trajectory n (m^3) in dependency of the water level $h_{s,n}$. For deriving the storage function we assume a constant cross-section within a trajectory. The function also includes the ‘added storage’ in the ditches that are connected to it within a subcatchment (Figure 3). An example is given in Figure 22.

In the model implementation we make the assumption that at the end of each trajectory there is a *unique* relationship between the water level and the flow rate. This relationship in the form of a metafunction is denoted by:

$$Q_n = \Theta_n(h_{s,n}) \quad (72)$$

where Q_n (value) and Θ_n ($h_{s,n}$) (function) are the outflow ($\text{m}^3 \text{s}^{-1}$) from trajectory n .

The metafunction $\Theta(b_{s,n})$ can be obtained in various ways, depending on:

- whether there is a weir or other structure at the end of the trajectory;
- whether or not a hydraulic model is used for deriving the metafunctions.

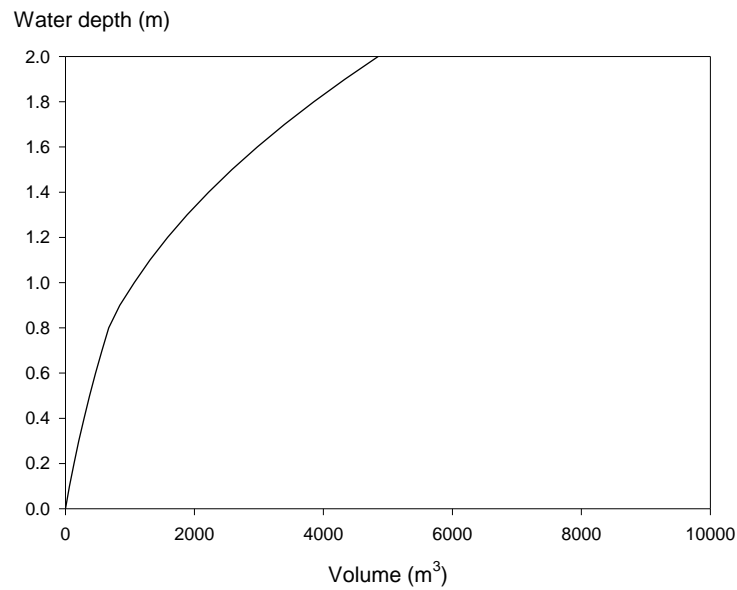


Figure 22 Example of a storage function for a trajectory (bottom width 2 m, side slopes 1:1, length 300 m), with ditches entering the watercourse at a height of 0.8 m (bottom depth of ditches 0.5 m, side slopes 1:1, total length of ditches within subcatchment 1200 m).

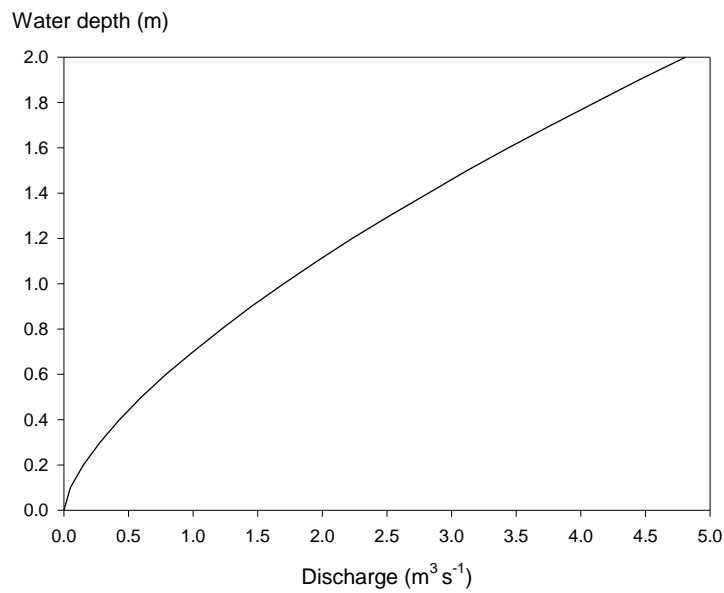


Figure 23 Example of a discharge function for a trajectory (rectangular short-crested weir with a crest width of 1 m, see Eq. 73)

5.3.1.1 Structures

For structures like weirs and culverts it is possible to use the special relationships describing the flow. For a simple rectangular short-crested weir, for instance, one can use (see Figure 23 for an example):

$$\Theta_n(h_{s,n}) = 1.7w(h_{s,n} - h_c)^{1.5} \quad (73)$$

where

$h_{s,n}$ = water level in trajectory n (m)

h_c = elevation of weir crest (m)

1.7 = weir coefficient (dependent on the type of weir) ($\text{m}^{0.5} \text{s}^{-1}$)

w = width of weir crest (m)

For the management of the crest level the model can employ several types of operational rules, as described in §6.3.1. In the case of a partially submerged weir the flow becomes less than what is given by Eq. 73: both the discharge coefficient and the exponent are influenced by the downstream water level. But to stay within the limitations of the model code we approximate the flow reduction by inserting the downstream water level $h_{s,n+1}$ in Eq. 73, instead of h_c . Another simplified representation of reality is that if the upstream water level rises above the soil surface next to the weir, the water involved in the excess head is assumed to flow freely to the next trajectory.

For a culvert, the relationship is given in terms of the head *difference*:

$$\Theta_n(h_{s,n}, h_{s,n+1}) = c\sqrt{(h_{s,n} - h_{s,n+1})} \quad (74)$$

where $h_{s,n+1}$ is the water level in the trajectory downstream of trajectory n , and c is a discharge coefficient ($\text{m}^{2.5} \text{s}^{-1}$) depending on the hydrodynamic properties of the culvert and the in- and outlet design. In situations with the downstream water level below the bottom of the culvert, the bottom-level h_c is used instead of $h_{s,n+1}$.

5.3.1.2 Open water conduits

For trajectories with unobstructed channel flow the simplest way of deriving the metafunctions is by assuming that the flow is uniform and that the influence of the trajectories on each other is negligible. By the latter is meant that the flow in the trajectories is not influenced by any backwater effects. This method is implemented by using the Chézy formula (made explicit by setting $dy/dx=0$ in Eq. 68) independently for each of the trajectories. But in many cases this simplification is inadequate. Then the preferred way of deriving the metafunctions is by performing computational experiments with a hydraulic model. In an example (Hermans *et al.*, 2004) using SOBEK-CF (WL|Delft Hydraulics, 2001) the movable weirs were set to their lowest position. Subsequently, the weirs were introduced in SIMGRO using relationships as e.g. given in Eq. 73.

A more sophisticated way of generating the metafunctions is to include the *management* of the weirs in the hydraulic model with which the experiments are made. The disadvantage of that method is, however, that each new water management strategy requires doing the

computational experiments anew. Another point is that the spatial distribution of the lateral inflow cannot be accurately foreseen without running the SIMGRO-model first. So of course the metamodeling of surface water has its limitations. In addition, to avoid anomalies in the simulation results, various amendments have been made to the model implementation, as described in §5.3.2.

5.3.2 Dynamics of channel flow

5.3.2.1 Solution scheme

The water balance of a trajectory is written as

$$S_n^{j+1} + \int_{t_s}^{t_s + \Delta t_s} Q_{out,n}(t) dt = S_n^j + \int_{t_s}^{t_s + \Delta t_s} [Q_{in,n}(t) + Q_{lat,n}(t)] dt \quad (75)$$

where:

- S_n^j = storage in trajectory n at time level j (m^3)
- $Q_{out,n}(t)$ = outflow of trajectory n ($m^3 d^{-1}$)
- $Q_{in,n}(t)$ = upstream inflow of trajectory n ($m^3 d^{-1}$)
- $Q_{lat,n}(t)$ = lateral inflow of trajectory n ($m^3 d^{-1}$)

The lateral inflow can be composed of several terms, which can also include extractions. The assumption is that these terms are evenly distributed along a trajectory, so that this also holds for the net inflow given by Q_{lat} .

Solving for the new water levels and discharges is done in two major steps:

- initially the assumption is made that the outflow from a trajectory (and also the flow direction) is uniquely defined for a certain water level, by the outflow metafunction Θ as given in Eq. 72 (or Eq. 73/74);
- the obtained solution is then checked for hydraulic anomalies (like flow to a trajectory having a higher water level), and if necessary it is corrected.

Given the assumption in the first solution step that the outflow from a trajectory is uniquely defined for a certain water level, it is possible to solve Eq. 75 for each trajectory separately, starting from the upstream end to ensure that the solution is based on the updated value of Q_{in} . In the case that the outflow metafunction Θ is given as Eq. 74, the downstream water level of the preceding time step is used as the second argument. For discharge pumps (§6.3.3), the on/off setting is determined at the start of the time step. If a surface water supply link is active (§6.3.2) the extraction and supply rate are also determined at the beginning of the time step. For the integration of Q_{out} within the time step we use a fully implicit scheme, because it is numerically more stable than a Crank-Nicholson weighting. The water balance equation is therefore used in the form:

$$S_n^{j+1} + Q_{out,n}^{j+1} \Delta t_s = S_n^j + [Q_{in,n}^{ave} + Q_{R,n}^{ave} + Q_{D,n}^{ave} - Q_{S,n}^{ave} - Q_{E,n}^{ave} + Q_{I,n}^{ave} + Q_{U,n}^{ave}] \Delta t_s \quad (76)$$

where:

- S_n^{j+1} = storage in trajectory n at time level $j+1$ (m^3)
 $Q_{\text{out},n}^{j+1}$ = outflow of trajectory n at time level $j+1$ ($\text{m}^3 \text{d}^{-1}$)
 $Q_{\text{in},n}^{\text{ave}}$ = upstream inflow of trajectory n , time averaged ($\text{m}^3 \text{d}^{-1}$)
 $Q_{\text{R},n}^{\text{ave}}$ = surface runoff to the trajectory n , time averaged ($\text{m}^3 \text{d}^{-1}$)
 $Q_{\text{D},n}^{\text{ave}}$ = drainage to (or infiltration from) the trajectory n , time averaged ($\text{m}^3 \text{d}^{-1}$)
 $Q_{\text{S},n}^{\text{ave}}$ = extraction of water for sprinkling from trajectory n , time averaged ($\text{m}^3 \text{d}^{-1}$)
 $Q_{\text{E},n}^{\text{ave}}$ = extraction of water for water supply to another trajectory ($\text{m}^3 \text{d}^{-1}$)
 $Q_{\text{I},n}^{\text{ave}}$ = inflow of water supply from another trajectory, using a special link ($\text{m}^3 \text{d}^{-1}$)
 $Q_{\text{U},n}^{\text{ave}}$ = inflow of water after being processed in a sewage plant ($\text{m}^3 \text{d}^{-1}$)
 Δt_s = time step (d)

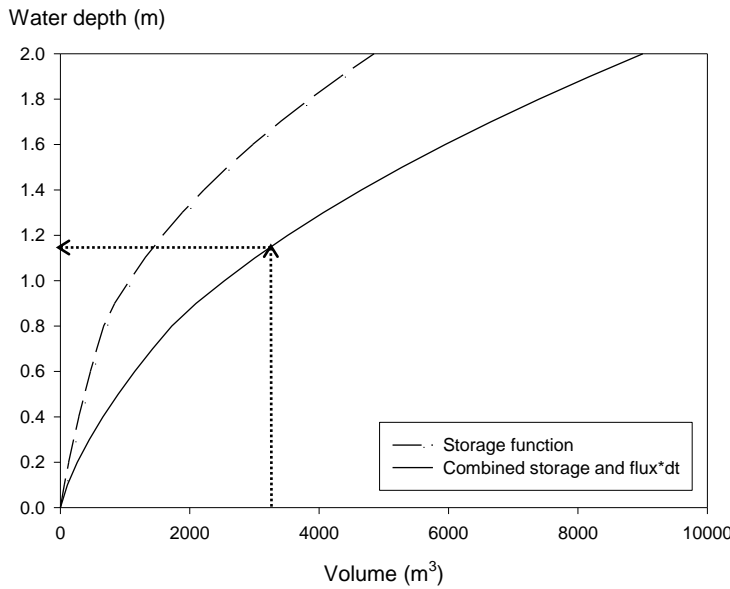


Figure 24 Combined storage and $\text{flux} \cdot dt$ function (Eq. 77, $dt=0.01 \text{ d}$) used in solving for the unknown water level and outflow: starting from the evaluated value using Eq. 76 the new water level is found by the inverse table interpolation following the arrow; the outflow is then given by the function shown in Figure 23.

The surface water system can be highly dynamic, so the time step should be chosen accordingly. Typical values used in the implementation of the model are 0.005 – 0.05 d.

No term is included for the precipitation/evaporation, in order to avoid double counting with the soil-water submodel. We assume that large tracts of surface water are modelled as ‘visible’ groundwater, with the watercourses simply serving as links to the rest of the network.

For efficient solving of Eq. 76 we prepare a combined storage-flux function (Figure 24) in the form of a table at programme initialization:

$$\sigma_n(h_{s,n}) = \Xi_n(h_{s,n}) + \Theta_n(h_{s,n}) \Delta t_s \quad (77)$$

For solving Eq. 76 its right-hand side is first evaluated. The solution for $h_{s,n}$ is then found through an inverse table interpolation of the storage-flux function (arrows in Figure 24).

This yields new values for the water level *and* for the outflow (after inserting the new water level in Eq. 72).

It is possible that the outflow from a trajectory n is split at a bifurcation (Figure 25). In that case the $\Theta(h_s)$ -function given by Eq. 72 is a summation of the flows to the manifold downstream trajectories of n . After having computed the new water level and the new outflow, the outflow is divided over the downstream branches according to the $\Theta_{n,n+1}(h_s)$ -functions of the separate trajectories diverging from the bifurcation.

The explicit nature of the over-all solution scheme can lead to instabilities, because the levels in the trajectories are solved one-by-one and not as a set. The latter method is customary in hydraulic models, which is inherently more stable. However, the disadvantage of solving a set of equations is the required computational effort. In SIMGRO an alternative way of stabilizing the levels is employed. In the case that the water level wants to rise faster than a pre-set maximum rate (Δh_{\max}), the surplus volume is computed and then temporarily stored. All of this volume is then added to the water balance for the next time step (as an extra term added to Eq. 76). In Figure 26 an example is given of the simulation with and without the described stabilization, for point c of Figure 25. From that example it becomes clear that the stabilization is not equivalent to a smoothing operation. In this case the over-all model stabilization affects the distribution of the discharge at the upstream bifurcation (point b), leading to a systematic shift in the discharge that passes the weir at c .

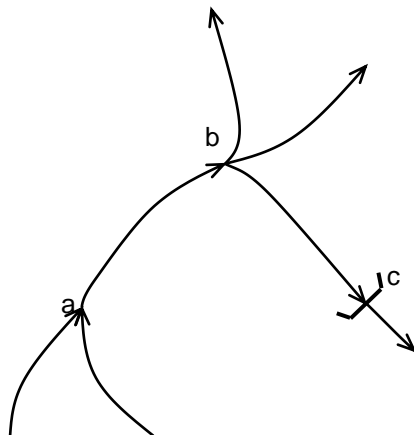


Figure 25 Example of a confluence (a) a bifurcation (b), and a weir (c)

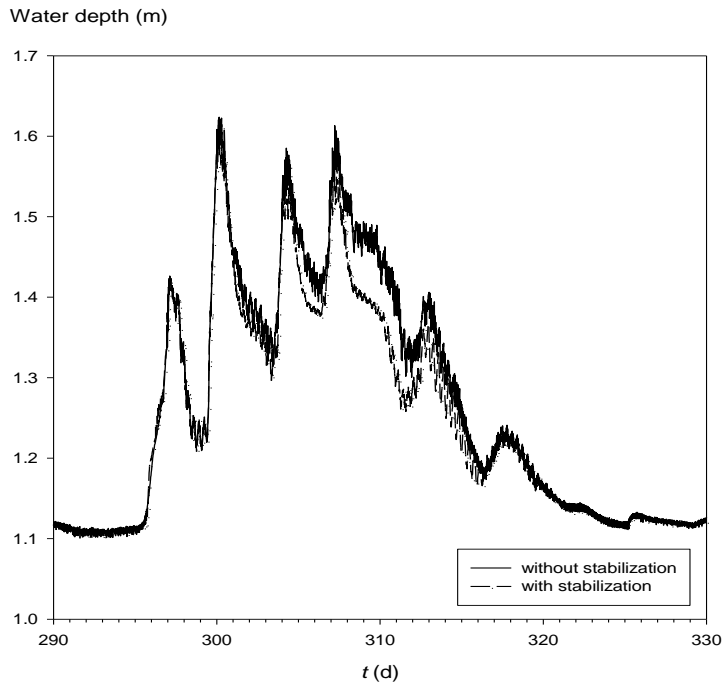


Figure 20 Example of a simulation run without the stabilization of the explicit calculation scheme. The systematic shift is due to the presence of a bifurcation upstream from the location for which the results are shown. The distribution of water over the branches of that bifurcation is affected by the over-all model stabilization, leading to a lower discharge in this case

5.3.2.2 Amendments

Before accepting the new discharge and water level as the final solution, a number of checks are made. Modifications are needed in the following instances, which are further explained in the subsequent paragraphs:

- in the presence of a hydraulic structure, and the computed water level becoming higher than the top of the structure, leading to an overflow situation;
- in the presence of an automated weir, with the computed level lower than the target level (see also §6.3.1);
- if the level is lower than the downstream level;
- in the presence of a bifurcation and a higher water level ('flow blocking') in one or more of the branches.

In the presence of a hydraulic structure that gets overflowed (see H_{constr} in Figure 35), the surplus volume is computed and then added to the outflow. The new water level is made exactly equal to the construction height.

In the presence of an automated weir a check is made to see if the target level is reached. If not, part of the outflow is used for filling up until the target level. It can happen that there is not enough water for doing this; the new water level will then be lower than the target, and the outflow is set to zero.

In the case that the downstream water level would otherwise become higher than the upstream one, the flow is temporarily 'put on hold', or the direction is even reversed. For this 'reverse flow' we assume that the friction is zero, because it usually will involve only relatively small flow rates, that are fed by water supply during dry periods (§6.3.2). The frictionless moving of water can be hampered by the discharge function. That is

especially relevant if there is an obstruction in the watercourse, like a weir or a culvert (Eq. 73 and 74). Such a situation is taken into account by assuming that the same discharge relationship also holds for flow in the reverse direction, with the up- and downstream levels changed around.

A special case of flow blocking can occur at a bifurcation if in one or more of the downstream branches the water level becomes higher than that in the upstream trajectory. If this occurs the flow to such a branch is (temporarily) set to zero, and divided proportionally over the remaining branches. If *all* of the branches have water levels higher than the upstream one, yet another dividing mechanism is brought into action:

- part of the flow is used for raising the water level in the upstream trajectory to that of the *lowest* level in the downstream branches;
- the remaining part of the flow is sent to the branch with the *lowest* water level.

If there is a water demand due to infiltration or sprinkling from surface water, then the model ascertains to which degree the demand can be fulfilled without causing a water balance error due to the falling dry of a trajectory. This demand realization is communicated back to the top system model of the soil/groundwater column, as explained in §1.

5.3.3 Water on the soil surface

The amount of water in storage on the soil surface is updated in a number of steps. The method is graphically illustrated in a sequence of figures. In Figure 27 a sketch is given of the schematization within a surface water unit. In the example the SVAT-unit has been made equal to the grid cell of the groundwater model. In Figure 28 the update for the ponding water processes (§**Error! Reference source not found.** and §3.2) is shown; there is a net loss due to evaporation. But this could of course just as well have been a net gain due to a precipitation event. The ‘control’ over the water on the soil surface is then passed to the surface water model. At the beginning of the time step an equalization takes place of the varying levels within the SVAT-units: the water on the soil surface is modelled as a reservoir with no horizontal head gradients within the surface water unit. This step is shown in Figure 29. After this equalization the actual surface water update takes place, which in the example of Figure 30 involves a water level drop due a net river outflow. This sequence of updates is repeated for the time steps of the ‘fast cycle’ of Figure 5. The time step is concluded by the update of the groundwater model. The groundwater model is informed about the ‘ponding recharge’, i.e. the net water balance effect of ponding water processes and the surface water flow on the ‘visible groundwater’. In the example this involves a net water loss (Figure 31). The groundwater model subsequently computes a net infiltration of water at the soil surface. This ‘loss’ of ponding water is communicated to the ponding submodel at the beginning of the next ‘fast’ cycle, and so on.

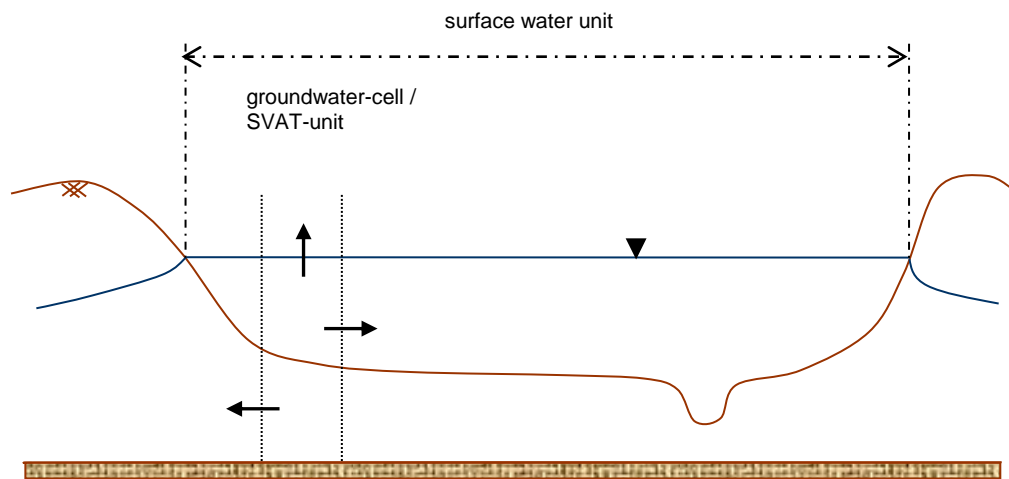


Figure 27 Schematisation of situation within a surface water unit

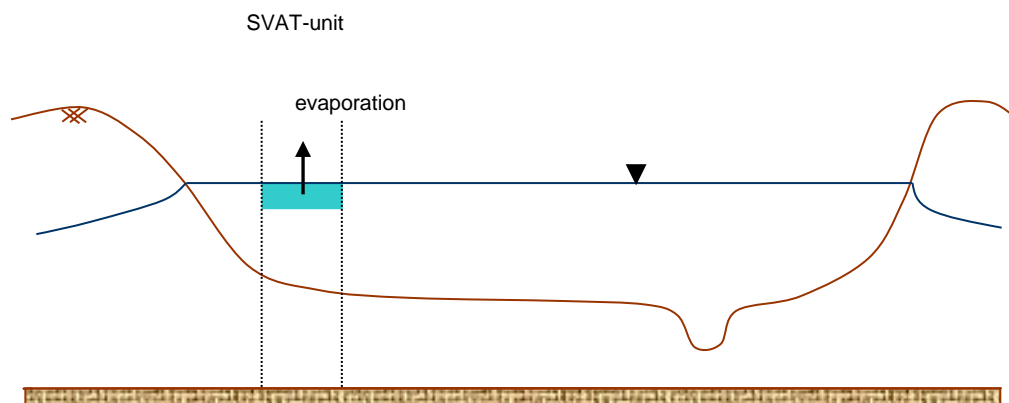


Figure 28 Situation after the update for ponding water processes, with a net evaporation in the example

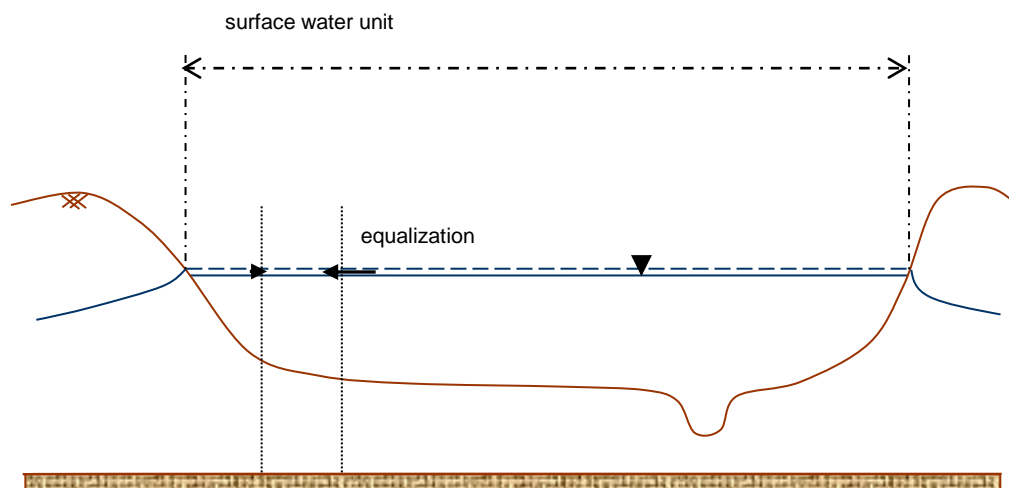


Figure 29 Situation after the update for the surface water equalization at the beginning of the surface water time step

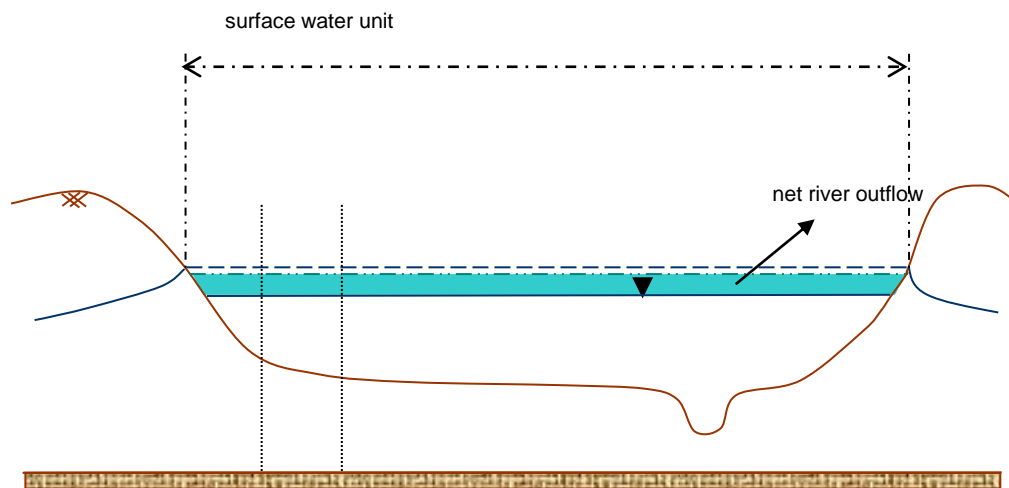


Figure 30 Situation after the update for the surface water simulation, in the example involving a net river outflow

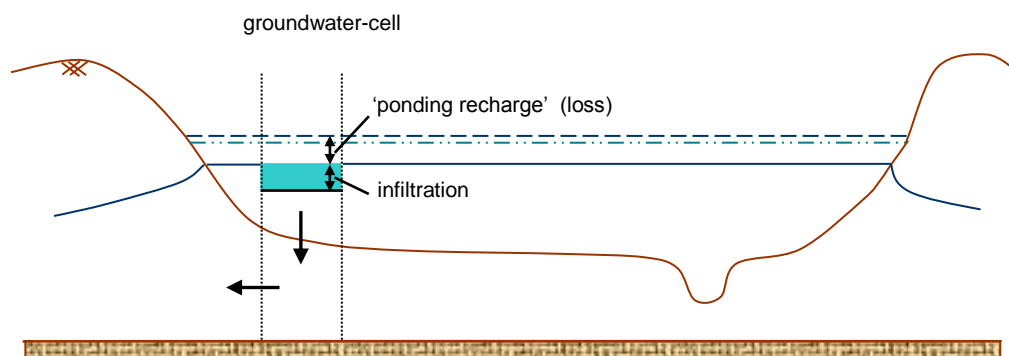


Figure 31 Situation after the update for the groundwater simulation, in the example involving a net infiltration

5.4 Data summary

For practical purposes the following classification into classes of watercourses is used:

- 1) primary watercourses, involving canals that traverse the region; the level is determined at a supra-regional scale, not in the model;
- 2) secondary watercourses, forming the main arteries of the regional system;
- 3) tertiary watercourses, usually the ditches;
- 4) tile drains;
- 5) gulleys/soil surface.

For each surface water trajectory that is explicitly modelled, there must be a specification of either:

- the discharge as a function of the water level (Eq. 72);
- the discharge as a function of the water level difference with the next trajectory (e.g. Eq. 74).

In the case of a bifurcation there can be several such functions for the flows to the multiple downstream branches.

For specifying the watercourse characteristics, each sub-section traversing a spatial unit must be specified in a list, with for each segment:

- the index of the system that is involved ($k=0,1,2,..5$); $k=0$ is reserved for trajectories that do not have any interaction in the form of drainage, but act only as a conduit for the surface water;
- the length of the segment;
- the cross-sectional specifications;
- the spatial unit involved;
- the surface water trajectory that the segment is connected with;
- the parameters defining the drainage resistance.

The use of this table involving the spatial units (instead of a table for the complete trajectories themselves) ensures consistency in the model. The parameters are here used for making tables of the storage function for the main watercourse (Eq. 71). In the groundwater model they are used for the drainage characteristics.

6 Water management

6.1 Introduction

Water management covers many features that have been discussed in the preceding chapters. For instance a small waterway that has been dug as a ditch is of course ‘non-natural’. Its dimensioning is part of the water management scheme. Water management is here defined to cover those parts of the system that do not have a pendant in the natural world. A fixed weir, for instance, is analogous to a dam-like obstruction in a river. Accordingly, its modelling has been discussed in §5. A weir that has a movable crest, on the other hand, is distinctly non-natural and therefore discussed below.

6.2 Land use

6.2.1 Urban areas

The water management of urban areas has evolved in the course of time. Originally it was just a question of discharging the rain and sewage water to the surroundings. But untreated water led to the spreading of diseases and to eutrophication. This has largely been remedied by building treatment plants. Recently the focus has further broadened. Whereas in the past urban areas were often considered as a ‘separate world’ from the surrounding rural area, there is now an increasing awareness that modern water management should be based on an integrated vision. The scheme given in Figure 32 is completely constructed from the generic model elements of SVAT-units described in §2 and §3 and the surface water elements described in §5.

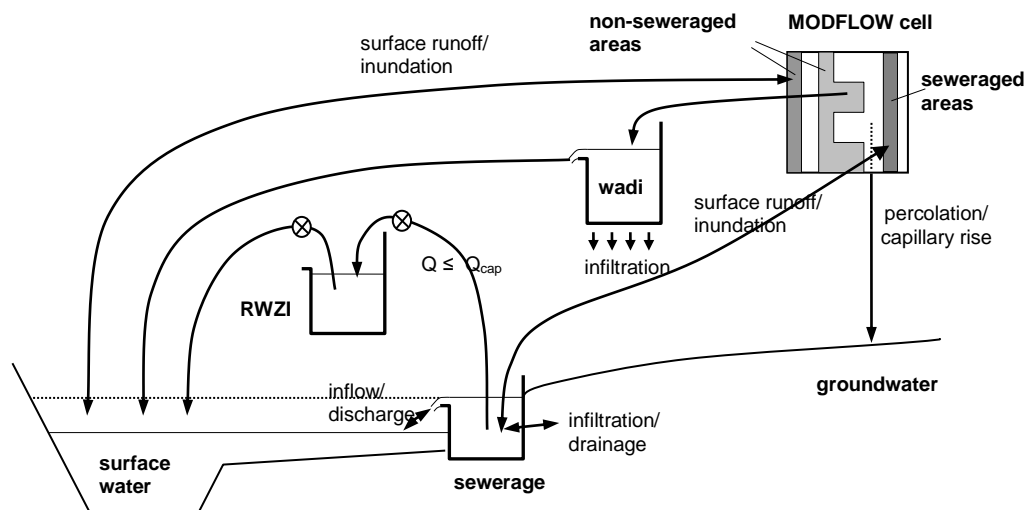


Figure 32 Schematic diagram of storage elements and transmission links in urban areas. An RWZI is a water treatment plant.

6.2.2 Sprinkled crops

During the growing season, precipitation deficits are likely to occur regularly. If the water content of the root zone drops below the reduction point (cf. **Error! Reference source not found.**), crop growth will be reduced. To avoid this, crops may be irrigated. In the Netherlands, sprinkler irrigation is the most common method. Depending on availability and legislation, sprinkling is done from surface water and/or groundwater.

In terms of water use efficiency, the performance of sprinkling systems is comparatively poor. Water losses due to runoff or percolation to the groundwater may be caused by:

- poor timing of sprinkling;
- poor dosing of sprinkling;
- sprinkling irregularities;
- installation leakage.

Additional losses are introduced by wind, evaporation and interception.

Sprinkling requirements are determined for each nodal subdomain and land-use type, for each time step of the soil water/groundwater model. SIMGRO allows the user to specify a sprinkling gift that may be applied with a rotational period. For determining the moment to start sprinkling use is made of the mean pressure head in the root zone. Sprinkling is triggered when this mean pressure head has fallen below a crop-related 'start' value, and discontinued as soon as it exceeds the 'stop' value. Case studies, carried out with this modelling concept have shown that these assumptions cause realistic amounts of sprinkling water to be simulated (Querner and Van Bakel, 1989).

The actual sprinkling gift is determined by both demand and capacity, as

$$Q_s = \min(Q_{s,\text{dem}}; Q_{s,\text{cap}}) \quad (78)$$

where

$$Q_{s,\text{dem}} = \text{sprinkling demand (m}^3 \text{ d}^{-1}\text{)}$$

$$Q_{s,\text{cap}} = \text{sprinkling capacity (m}^3 \text{ d}^{-1}\text{)}$$

If sprinkling from both groundwater and surface water are enabled, sprinkling from surface water has priority. The total sprinkling capacity is calculated as:

$$Q_{s,\text{cap}} = Q_{s,\text{cap}}^g + Q_{s,\text{cap}}^s \quad (79)$$

where:

$$Q_{s,\text{cap}}^g = \text{sprinkling capacity from groundwater (m}^3 \text{ d}^{-1}\text{)}$$

$$Q_{s,\text{cap}}^s = \text{sprinkling capacity from surface water (m}^3 \text{ d}^{-1}\text{)}$$

The groundwater extraction capacity is not considered time dependent, or dependent on the groundwater conditions. Thus the capacity is simply an input parameter. The maximum possible extraction of surface water depends on the prevailing surface water conditions. Below a certain critical water level the sprinkling is discontinued. In order to effectuate this in the model without causing a water balance violation at the moment that the surface water runs dry (or drops below a critical level), the sprinkling water is ‘collected’ during the preceding time step of the groundwater model, and held in storage until the next one. This algorithm suffices for the time steps of less than 1 d that are usually used in SIMGRO.

During sprinkling the atmospheric conditions are usually hot, as opposed to conditions that often prevail when there is natural rainfall. Under normal conditions the rainfall of course also evaporates as it falls. However, that has already been discounted: only the rain that actually reaches the ground surface is measured at the gauging station. Therefore, the evaporation of natural rainfall is not accounted for in the model. With respect to the sprinkling water we assume that a certain fraction is lost to evaporation. That is handled as a separate term in the computation of the evapotranspiration, for which no discounting is done with respect to the reference crop evapotranspiration:

$$ET_{act,spr} = f_{spr} Q_s / A_i; \quad P_{s,net} = (1 - f_{spr}) Q_s / A_i \quad (80)$$

where

- $ET_{act,spr}$ = amount of sprinkling water that directly evaporates before reaching the vegetated (soil) surface, per unit area of SVAT ($m\ d^{-1}$)
- f_{spr} (-) = fraction of the sprinkling water that is lost to evaporation (-)
- A_i = area of nodal subdomain (m^2)
- $P_{s,net}$ = the net sprinkling intensity ($m\ d^{-1}$)

6.3 Surface water

6.3.1 Weirs

Weirs can have advanced technology, including a radio-link to a monitoring point. An automated weir has an electro-mechanical gadget for adjusting the height of the crest, which can be programmed for achieving a target level at either the upstream or downstream side. An upstream control weir can for instance be used in conjunction with groundwater management. For that purpose the SIMGRO-code has the possibility of letting the weir/target level settings be determined by groundwater conditions at a monitoring point. Then a weir control scheme must be specified in the form of a piece-wise linear function, with per record:

- a groundwater level in the monitoring point i ;
- a target level (or crest level) in trajectory n .

An example of a target-level control function is given in Figure 33a. The aim of that scheme is to achieve ideal conditions for crop growth (Van Walsum and Van Bakel, 1983; Van Bakel, 1986). In this case the 'ideal' groundwater level is thought to be 4.7 m +MSL, the point where the dashed line (1:1) intersects the function. For groundwater levels higher than the ideal one, the target level is lowered in an attempt to bring the groundwater level down; for groundwater levels lower than the ideal one, the target level is raised.

An example of a downstream control scheme is given in Figure 33b: if the downstream level starts to drop below 1.6 m +MSL, the crest level in the upstream trajectory is lowered in an attempt to maintain the desired water level. Such a type of

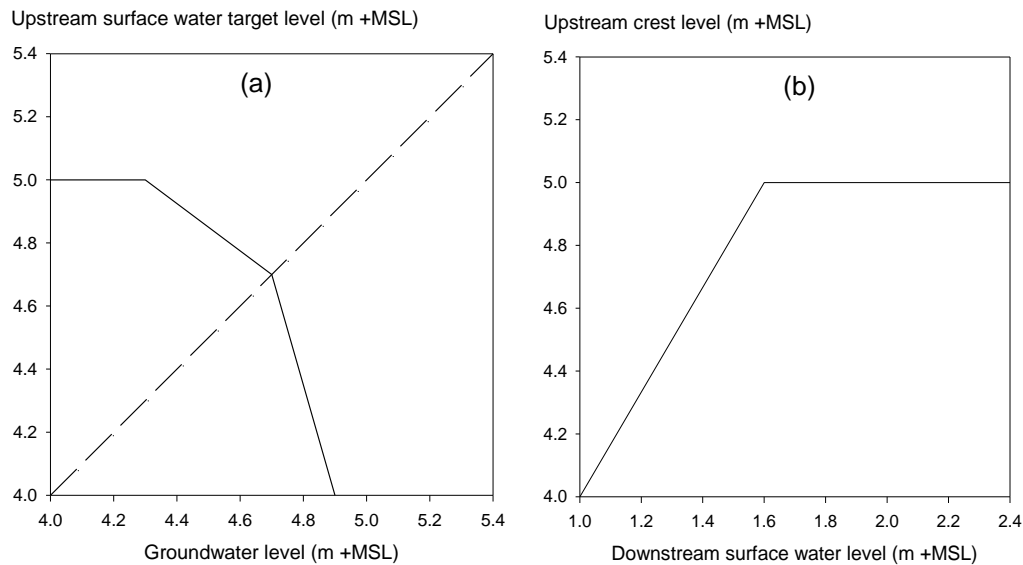


Figure 33 Weir management schemes: a) upstream control based on groundwater monitoring, aimed at optimizing conditions for crop production (soil surface at 5.4 m +MSL); b) downstream control based on surface water monitoring, aimed at stabilizing a downstream water level

scheme is commonly used for regulating demand-driven water supply in an irrigation channel network. But surface water supply can also be needed for maintaining water quality by forcing a certain amount of throughflow, for flushing the system. Then a different kind of control is needed as described in the next paragraph.

6.3.2 Surface water supply links

In SIMGRO it has been made possible to establish special links that involve water transfer from one watercourse to the next, as shown in Figure 34. Such a link does not have to involve an existing connection in the network that is used for calculating the discharge dynamics as described in §5.3.2; neither is there any constraint on creating ‘closed circuits’ in the network in this manner. (Closed circuits are not allowed for the discharge dynamics, because the algorithm requires a strict upstream to downstream calculation order). No storage is taken into account in the link itself. So in order to remain realistic it should not be very long.

The flow regulation is based upon stepwise adjustment of the supply rate, at each time step of the surface water model (cf. Figure 34). The used increments and decrements are $[\Delta t_s / \Delta t_g] \cdot [\text{supply capacity}]$. So the full supply capacity can be reached at the end of the first groundwater time step. The flow rate is *decremented* if one (or more) of the following conditions are present:

- the water level in the extraction trajectory n has become lower than the allowed depletion level;
- the water level in the supply trajectory m has exceeded the maximum allowed level;
- the flow rate at the flow control trajectory k is higher than the target flow.

The flow rate is *incremented* if *none* of the above conditions and one (or more) of the following conditions are present:

- the flow rate at the flow control trajectory k is lower than the target flow;
- the water level in the supply trajectory m is lower than the maximum allowed level.

The flow rate is not allowed to exceed the specified capacity.

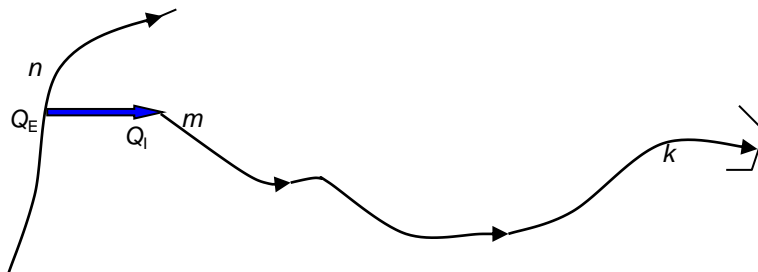


Figure 34 Surface water supply link. Water is transferred from trajectory n to m . Supply control is based on the water levels in n and m , and the flow over the weir at k .

The criterium for the depletion level of the the extraction trajectory is purely based on the available water in storage. So the algorithm does not take into account that there can be inflow to the extraction trajectory from e.g. an upstream trajectory. The amount of water that can be supplied in this manner is limited by the storage characteristics, the weir/target level and the allowed level of depletion in the extraction trajectory. This storage-related amount can be supplied at each time step of the surface water. So the realized supply flow rate can be increased by either increasing the storage capacity or by making the time step smaller.

6.3.3 Discharge pumps

For a pump the management can be specified in the form of a switch, with a ‘start-level’ and ‘stop-level’ (H_{start} and H_{stop} , Figure 35). If the water level rises above the construction height (H_{constr}), the water is free to move over the top. Such a construction height is also specified in the input data for weirs and culverts.

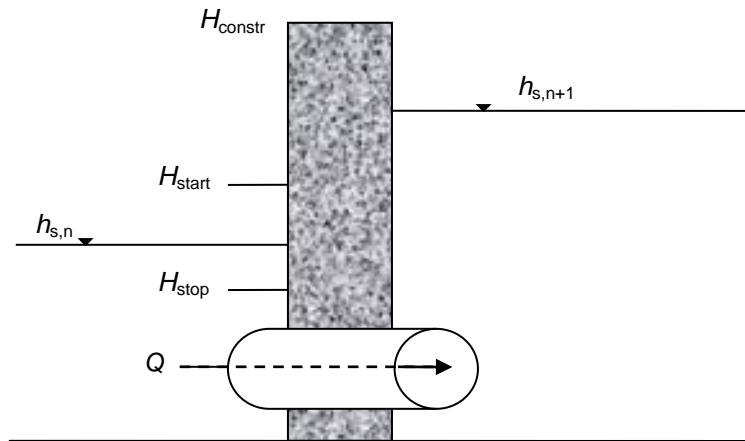


Figure 35 Pumping station, with a start and a stop level for switching the pump on and off. If the water level rises above the construction height H_{constr} , the structure overflows and the water is free to move over the top

References

- Allen, R.G., L.S. Pereira, D. Raes, and M. Smith, 1998. *Crop evapotranspiration. Guidelines for computing crop water requirements*. Irrigation and Drainage Paper 56, FAO, Rome, Italy, 300 p.
- Bear, J. 1977. *Hydraulics of groundwater*. Mc-Graw-Hill.
- Belmans, C., J.G. Wesseling and R.A. Feddes, 1983. *Simulation of the water balance of a cropped soil: SWATRE*. J. Hydrol., 63, 271-286.
- Boesten, J.J.T.I. and L. Stroosnijder, 1986. *Simple model for daily evaporation from fallow tilled soil under spring conditions in a temperate climate*. Neth. J. Agric. Sci., 34, 75-90.
- Crank, J. and P. Nicolson, 1947. *A practical method for numerical evaluation of solutions of partial differential equations of the heat-conduction type*. Proc. Camb Phil. Soc. 43: 50-67.
- De Bruin, H.A.R., 1987. *From Penman to Makkink*. Comm. Hydrol. Res. TNO, The Hague. Proc. and Inf. 39:5-31.
- De Laat, P.J.M., 1980. *Model for unsaturated flow above a shallow water table, applied to a regional subsurface flow problem*. Doctoral thesis, Agric. University Wageningen. Pudoc, Wageningen.
- Dumm, L.D. 1954. *Drain spacing formula*. Agr. Eng. 35: 726-730.
- Ernst, L.F. 1962. *Grondwaterstroming in de verzadigde zone en hun berekening bij aanwezigheid van horizontale evenwijdige open leidingen*. Wageningen, Ph.D thesis.
- Ernst, L.F., 1978. *Drainage of undulating sandy soils with high groundwater tables. I. A drainage formula based on a constant hydraulic head ratio. II. The variable hydraulic head ratio*. J. Hydrol. 39, 3/4:1-50.
- Ernst, L.F. *Wegzijing en kwel; de grondwaterstroming van hogere naar lagere gronden*. Rapport 7. Instituut voor Cultuurtechniek en Waterhuishouding, Wageningen.
- Feddes, R.A., P.J. Kowalik, and H. Zaradny, 1978. *Simulation of field water use and crop yields. Simulation monographs*. University of Wageningen, Pudoc.
- Feddes, R.A., 1987. *Crop factors in relation to Makkink reference- crop evapotranspiration*. Comm. Hydrol. Res. TNO, The Hague. Proc. and Inf. 39: 33-44.
- Feddes, R.A., P. Kabat, P.J.T. van Bakel, J.J.B. Bronswijk and J. Halbertsma, 1988. *Modelling soil water dynamics in the unsaturated zone - state of the art*. J. Hydrol. 100: 69-111.

Goudriaan, J., 1977. *Crop meteorology: a simulation study*. Simulation monographs, Pudoc, Wageningen.

HarmonIT. 2005. *The org.OpenMI.Standard interface specification. Part C of the OpenMI document Series*. IT frameworks (HarmonIT). EC-FP5 Contract EVK1-CT-2001-00090.

Hermans, A.G.M., P.E.V. van Walsum, J. Runhaar, & P.J.T. van Bakel. 2004. *Duurzaam waterbeheer Langbroekernivetering; Fase 1: Modelbouw, calibratie en bepaling van het Actueel Grond- en Oppervlaktewaterregime*. Wageningen, Alterra, Alterra-rapport 914.

Jensen, M.E., R.D. Burman and R.G. Allen, 1990. *Evapotranspiration and irrigation water requirements*. ASCE manuals and reports on engineering practice 70, ASCE, New York. 332 pp.

Jousma, G., and H.Th.L. Massop. 1996. *Intreeweerstanden; inventarisatie en analyse*. TNO-grondwater en Energie, Delft. Rapport GG-R-96-15(A).

Kraijenhoff van de Leur, D.A. 1958. *A study of non-steady groundwater flow with special reference to a reservoir coefficient*. De Ingenieur, 70, B87–B94.

Kroes, J.G., J.C. van Dam, P. Groenendijk, R.F.A. Hendriks, and C.M.J. Jacobs. 2008. *SWAP version 3.2; Theory description and user manual*. Wageningen, Alterra-report 1649, Alterra.

Molen, W.H. van der. 1972. *Waterbeheersing (collegdictaat)*. Wageningen, Vakgroep Cultuurtechniek..

Monteith, J.L., 1965. *Evaporation and the Environment*. In: G.E. Fogg (ed.), *The state and movement of water in living organisms*. Cambridge University Press, p. 205-234.

Monteith, J.L., 1981. *Evaporation and surface temperature*. Quarterly J. Royal Soc., 107, 1-27.

Penman, H.L., 1948. *Natural evaporation from open water, bare soil, and grass*. Proc. Royal Society, London 193, 120-146.

Prasad, R. 1988. *A linear root-water-uptake model*. J. Hydrol. 99: 297–306

Querner, E.P. , 1988. *Description of a regional groundwater flow model SIMGRO and some applications*. Agric. Water Man. 14: 209-218.

Querner, E.P. and P.J.T. van Bakel, 1989. *Description of the regional groundwater flow model SIMGRO*. Wageningen, DLO-Staring Centrum, Report 7.

Richards, L.A., 1931. *Capillary conduction of liquids through porous mediums*. Physics 1: 318:333.

Rijtema, P.E. 1965. *An analysis of actual evapotranspiration*. Agricultural Reports 659. PUDOC, Wageningen. 107 pp.

Ritchie, J.T., 1972. *A model for predicting evaporation from a row crop with incomplete cover*. Water Resour. Res., 8, 1204-1213.

Rutter, A.J., K.A. Kershaw, P.C. Robins, and A.J. Morton, 1971. *A predictive model of rainfall interception in forests, 1. Derivation of the model from observations in a plantation of Corsican Pine*. Agr. Meteor. 9: 367-384.

Valente, F., J.S. David, and J.H.C. Gash. 1997. *Modelling interception loss for two sparse eucalypt and pine forests in central Portugal using reformulated Rutter and Gash analytical models*. J. of Hydrol., 190, 141-162.

Van Bakel, P.J.T. 1986. *A systematic approach to improve the planning, design and operation of surface water management systems: a case study*. Wageningen, Ph. D. thesis.

Van Walsum, P.E.V. and P.J.T. van Bakel, 1983. *Berekening van de effecten van infiltratie op de gewasverdamping in het herinrichtingsgebied, met een aangepaste versie van het model SWATRE*. Wageningen, Instituut voor Cultuurtechniek en Waterhuishouding, Nota 1434.

Van Walsum, P.E.V. and P. Groenendijk, 2008. *Quasi steady-state simulation of the unsaturated zone in groundwater modeling of lowland regions*. Vadose Zone Journal 7:769-781.

Veldhuizen, A.A., A. Poelman, L.C.P.M. Stuyt and E.P. Querner. 1998. *Software documentation for SIMGRO V3.0; Regional water management simulator*. Technical Document 50. SC-DLO, Wageningen.

Veldhuizen, A.A., P.E.V. van Walsum, A. Lourens, P.E. Dik. 2006. *Flexible integrated modeling of groundwater, soil water and surface water*. Proceedings of MODFLOW 2006 (p. 94 -98). IGWMC, Colorado.

Chow, V.T. 1959. *Open-channel hydraulics*. McGraw-Hill, New York.

Wesseling, J. 1957. *Enige aspecten van de waterbeheersing in landbouwgronden*. Ph. D. thesis. Versl. van Landbouwk. Onderz. 63.5. Pudoc, Wageningen.

WL | Delft Hydraulics, 2001. *SOBEK Rural, managing your flow*. Manual version 2.07, WL| Delft Hydraulics, Delft.

Wosten, J.H.M., G.J. Veerman, W.J.M. de Groot, J. Stolte. 2001. *Waterretentie- en doorlatendheidskarakteristieken van boven- en ondergronden in Nederland: de Staringreeks*. Vernieuwde uitgave 2001. Alterra-rapport 152. Alterra, Wageningen.

Appendix A Steady-state unsaturated flow simulations

The soil physical parameters are not used in a direct way. In the pre-processing stage they are converted to ‘metafunctions’ for the capillary rise /percolation flux density and the storage in the subsoil. These functions are derived by making a series of steady-state simulations with a special version of the SWAP model (Kroes et al., 2008). In the steady-state simulations of moisture profiles, the conductivity variable is treated in an implicit manner whereas in the original SWAP model this variable is treated explicitly. The analytical hydraulic conductivity relation as presented by Mualem (1976) is used where the classical soil moisture retention relationship of Van Genuchten (1980) has been applied to calculate the saturation degree:

$$k(\psi) = k_{\text{sat}} \frac{\left[\left(1 + |\alpha\psi|^n \right)^m - |\alpha\psi|^{n-1} \right]^2}{\left(1 + |\alpha\psi|^n \right)^{m(\lambda+2)}} \quad (81)$$

where k_{sat} is the saturated conductivity (m d^{-1}) and α (m^{-1}), n (-) and m (-) are empirical shape factors where $m=1-1/n$. The derivative of the conductivity k to the pressure head ψ is given by:

$$\frac{\partial k}{\partial \psi} = \left| -\frac{\lambda}{\psi} \frac{m}{1 + |\alpha\psi|^n} \frac{|\alpha\psi|^n}{1 + |\alpha\psi|^n} k(\psi) \right| \quad (82)$$

Eq. 82 can be elaborated to finite increments. For soil compartment i the following condition holds:

$$F_i = k_{i-1/2} \left(\frac{\psi_{i-1} - \psi_i}{\frac{1}{2}(\Delta z_{i-1} + \Delta z_i)} + 1 \right) - k_{i+1/2} \left(\frac{\psi_i - \psi_{i+1}}{\frac{1}{2}(\Delta z_i + \Delta z_{i+1})} + 1 \right) - \Delta z_i Q_{a,i} \quad (83)$$

where F_i is the residual of the water balance of a certain compartment for a certain time level, $k_{i-1/2}$ and $k_{i+1/2}$ are internodal conductivities calculated as weighted arithmetic means of the nodal conductivities and Δz_{i-1} , Δz_i and Δz_{i+1} are compartment thicknesses.

The solution of the scheme implies a root-finding procedure which obeys to the prerequisite that the residual F_i should approach a zero value. A Newton Raphson-iteration scheme (Press, 1992) is employed to solve the set of non-linear equations:

$$\begin{pmatrix} \psi_1^{p+1} \\ \vdots \\ \psi_i^{p+1} \\ \vdots \\ \psi_n^{p+1} \end{pmatrix} = \begin{pmatrix} \psi_1^p \\ \vdots \\ \psi_i^p \\ \vdots \\ \psi_n^p \end{pmatrix} - \begin{pmatrix} \frac{\partial F_1}{\partial \psi_1^p} & \frac{\partial F_1}{\partial \psi_2^p} & 0 & 0 & 0 \\ \frac{\partial F_2}{\partial \psi_1^p} & \frac{\partial F_2}{\partial \psi_2^p} & \dots & 0 & 0 \\ 0 & \frac{\partial F_i}{\partial \psi_{i-1}^p} & \frac{\partial F_i}{\partial \psi_i^p} & \frac{\partial F_i}{\partial \psi_{i+1}^p} & 0 \\ 0 & 0 & \dots & \frac{\partial F_{n-1}}{\partial \psi_{n-1}^p} & \frac{\partial F_{n-1}}{\partial \psi_n^p} \\ 0 & 0 & 0 & \frac{\partial F_n}{\partial \psi_{n-1}^p} & \frac{\partial F_n}{\partial \psi_n^p} \end{pmatrix}^{-1} \begin{pmatrix} F_1 \\ \vdots \\ F_i \\ \vdots \\ F_n \end{pmatrix} \quad (84)$$

where the superscript $p+1$ points to the solution of iteration cycle p . The starting values are indicated by the superscript p . The coefficients of the Jacobian are given by:

$$\begin{aligned}
\frac{\partial F_i^p}{\partial \psi_{i-1}^p} &= \frac{k_{i-1}^p \Delta z_{i-1} + k_i^p \Delta z_i}{\frac{1}{2}(\Delta z_{i-1} + \Delta z_i)^2} + \left(\frac{\psi_{i-1}^p - \psi_i^p}{\frac{1}{2}(\Delta z_{i-1} + \Delta z_i)} + 1 \right) \frac{\Delta z_{i-1}}{\Delta z_{i-1} + \Delta z_i} \frac{\partial k_{i-1}^p}{\partial \psi_{i-1}^p} \\
\frac{\partial F_i}{\partial \psi_i^p} &= -\frac{k_{i-1}^p \Delta z_{i-1} + k_i^p \Delta z_i}{\frac{1}{2}(\Delta z_{i-1} + \Delta z_i)^2} - \frac{k_i^p \Delta z_i + k_{i+1}^p \Delta z_{i+1}}{\frac{1}{2}(\Delta z_i + \Delta z_{i+1})^2} + \left(\frac{\psi_{i-1}^p - \psi_i^p}{\frac{1}{2}(\Delta z_{i-1} + \Delta z_i)} + 1 \right) \frac{\Delta z_i}{\Delta z_{i-1} + \Delta z_i} \frac{\partial k_i^p}{\partial \psi_i^p} \\
&\quad - \left(\frac{\psi_i^p - \psi_{i+1}^p}{\frac{1}{2}(\Delta z_i + \Delta z_{i+1})} + 1 \right) \frac{\Delta z_i}{\Delta z_i + \Delta z_{i+1}} \frac{\partial k_i^p}{\partial \psi_i^p} - \Delta z_i \frac{\partial Q_{a,i}^p}{\partial \psi_i^p} \\
\frac{\partial F_i}{\partial \psi_{i+1}^p} &= \frac{k_i^p \Delta z_i + k_{i+1}^p \Delta z_{i+1}}{\frac{1}{2}(\Delta z_i + \Delta z_{i+1})^2} - \left(\frac{\psi_i^p - \psi_{i+1}^p}{\frac{1}{2}(\Delta z_i + \Delta z_{i+1})} + 1 \right) \frac{\Delta z_{i+1}}{\Delta z_i + \Delta z_{i+1}} \frac{\partial k_{i+1}^p}{\partial \psi_{i+1}^p}
\end{aligned} \quad (85)$$

The derivative of the root extraction sink term is approximated numerically. For each soil physical schematization a series of calculations is done in which the root zone depth (d_r), the phreatic level (h) and the flux density at the upper boundary are varied. The purpose of the computational experiments is to derive functions that cover the full range of conditions that can occur in a soil column, including the root zone. The maximum precipitation should be high enough to generate surface runoff, thus ensuring that the situation with maximum percolation is covered. The highest evapotranspiration rate should equal the highest possible value of the potential evapotranspiration. The root water uptake reduction function then plays a role in the determining the steady state situation that is reached. From the series of computational experiments the following tabular functions are derived for each soil physical schematization:

- $\mathbf{TB}_{s_1}(d_r, \psi_r, h)$: total storage of water in the root zone (control box 1), as function of the root zone thickness d_r , the mean root zone pressure head ψ_r and the ground-water level h (m);
- $\mathbf{TB}_{s_2}(d_r, \psi_r, h)$: total storage of water in the subsoil (control box 2)
- $\mathbf{TB}_{q_m}(d_r, \psi_r, h)$: moisture flux density of a steady-state profile (m d^{-1})